ISSN (Online): 2305-0225
Issue 15(4), August 2014, pp. 469-475

An Intuitionistic Fuzzy Model for Project Scheduling Under Uncertainty

Mohammad HoseinMahmoudi Sari1, Abdolvahed Ghaderi2,Mahdi Zowghi*3

1.Department of Civil Engineering, University of Tehran, Iran
2.Department ofEngineering andTechnology,Bircham International University , Spain
3.Department of Business and Management, Willington University

Abstract: The concept of an intuitionistic fuzzy set can be seen as an alternative approach to define a fuzzy set in cases where available information is not sufficient for the definition of an imprecise concept by means of a conventional fuzzy set. In this paper a new method based on intuitionistic fuzzy set is developed to solve the project scheduling problem. In this method we consider several project characteristics in uncertain environment such as durations and precedence links and analysis fuzzy critical path with computing forward and backward pass calculations. Through a numerical example, calculation steps inthis method and the results are illustrated.

Keywords: Intuitionistic Fuzzy Set, Project Scheduling, Uncertainty

1. Introduction

Scheduling is a very important part of the planning phase of project management. Several methods have been proposed for solving scheduling problems. These methods take the values of some parameters of the problem as the input and generate a schedule for the problem. In most of the cases, the parameters of the projects are estimated based on the domain knowledge and past experience of the manager. So there is some amount of uncertainty embedded in these estimates [3]. The classical project scheduling methods can't effectively handle these kinds of problems. Fuzzy set theory [4] based project scheduling methods can comfortably be used in the problems with such imprecise information. Out of several higher-order fuzzy sets, intuitionistic fuzzy sets introduced by Atanassov [5] have been found to be well suited to dealing with vagueness. The concept of an intuitionistic fuzzy set can be seen as an alternative approach to define a fuzzy set in cases where available information is not sufficient for the definition of an imprecise concept by means of a conventional fuzzy set. In general, the theory of intuitionistic fuzzy sets is the generalization of fuzzy sets. Therefore, intuitionistic fuzzy sets could be useful in simulating human decision making processes and any activities requiring human expertise and knowledge [1, 2]. To this end, several methods have been developed during the last four decades [9, 10, 11].The first method called FPERT was proposed by Chanas and Kamburowski[12]. In mentioned research the project completion time is given in the form of a fuzzy set in the time space, thenGazdik[13] developed a fuzzy network of an a priori unknown project to estimate the activity duration, and used fuzzy algebraic operators to calculate the duration of the project and its critical path. This work is called FNET. An extension of FNET was proposed by Nasution[14] and Lorterapong and Moselhi[15]. Following on this McCahon[16], Chang et al. [17] and, Lin and Yao [18] presented three methodologies to calculate the fuzzy completion project time. Other researchers such as Kuchta[19], Yao and Lin [20], Chanas and Zielinski [21]used fuzzy numbers and presented other methods to obtain fuzzy critical paths and critical activities and activity delay. Kaufmann and Gupta [22], Hapke et al. [7] ,Hapke and Slowinski [7] and Rommelfanger [7] proposed a backward recursion that relies on the optimistic fuzzysubtraction and they provided good results for particular networks but these methods fail to compute the fuzzy lateststarting times and floats in general networks. Nasution [23] resorts to symbolic computations on variable durationtimes. McCahon and Lee [16], Mon et al. [7] and Yao and Lin [16] proposed to go back to classical CPM viadefuzzification of the fuzzy durations. McCahon [16] proposed to compute approximated fuzzy floats of activitiesfrom the fuzzy starting times obtained by the forward and backward recursions. Chen and Hsueh [12] and Chen [18] proposed an approach based on the extension principle and linear programming formulation to critical path analysis in networks with fuzzy activity durations. Chen and Huang [12] combined fuzzy set theory with the traditional methods to compute the critical degrees of activities an paths. Instead of the traditional objective, minimizing the make-span of the project, Yakhchali and

ISSN (Online): 2305-0225
Issue 15(4), August 2014, pp. 469-475

Ghodsypour [22] discussed project scheduling problem with irregular starting time costs in networks with imprecise durations.

In this paper we have supposed duration of activities and preference relations are imprecise and showed in the form of intuitionistic fuzzy sets. The rest of the paper is structured as follows. In the next section we introduce the notations used in this paper and then we explain the problem in section 3. We discuss the proposed heuristic in section 4 and use that to solve a problem taken from the literature in section 5. Finally, we discuss the results, future research directions and then we conclude.

2. Definitions

Definition 1; A fuzzy set $\tilde{A}$ in a universe of discourse X is characterized by a membership function $\mu_{\tilde{A}}(X)$ which associates with each element x in X, a real number in the interval [0,1]. The function value $\mu_{\tilde{A}}(X)$ is termed the grade of membership of x in $\tilde{A}$ [4].

Definition 2; A linguistic variable is a variable whose values are expressed in linguistic terms [6]. The concept of a linguistic variable is very useful to describe situations that are too complex or not well defined in conventional quantitative expressions. For example, ‘‘weight” is a linguistic variable the values of which could be very low, low, medium, high, very high, etc.

Definition 3; An intuitionistic fuzzy set $\tilde{A}$ in X is given by

$$\tilde{A} = \{(x, \mu_{\tilde{A}}(X), \vartheta_{\tilde{A}}(X)) | x \in X\} \quad (1)$$

Where $\mu_{\tilde{A}}: X \to [0,1]$ and $\vartheta_{\tilde{A}}: X \to [0,1]$ with the condition $0 \le \mu_{\tilde{A}}(X) + \vartheta_{\tilde{A}}(X) \le 1 \quad \forall x \in X$. The numbers $\mu_{\tilde{A}}(X)$ and $\vartheta_{\tilde{A}}(X)$ represent the membership degree and non-membership degree of the element x to the set $\tilde{A}$.

Definition 4; for each an intuitionistic fuzzy set $\tilde{A}$in X, if

$$\pi_{\tilde{A}}(X) = 1 - \mu_{\tilde{A}}(X) - \vartheta_{\tilde{A}}(X) \forall x \in X \quad (2)$$

Then $\pi_{\tilde{A}}(X)$ is called the degree of indeterminacy of x to the set $\tilde{A}$.

Definition 5; A TIFN $\tilde{a} = \left\{\left(\underline{a}^{\mu}, a, \overline{a}^{\mu}; w_{\tilde{a}}\right), \left(\underline{a}^{\vartheta}, a, \overline{a}^{\vartheta}; u_{\tilde{a}}\right)\right\}$ is an IFS in $\mathbb{R}$, whose membership and non-membership functions are respectively defined as follows [8]:

$$\mu_{\tilde{a}}(x) = \begin{cases} \frac{(x - \underline{a}^{\mu}) w_{\tilde{a}}}{a - \underline{a}^{\mu}} & \underline{a}^{\mu} \le x < a \\ w_{\tilde{a}} & x = a \\ \frac{(\overline{a}^{\mu} - x) w_{\tilde{a}}}{\overline{a}^{\mu} - a} & a < x \le \overline{a}^{\mu} \\ 0 & othrewise, \end{cases}$$

$$\vartheta_{\tilde{a}}(x) = \begin{cases} \frac{a - x + (x - \underline{a}^{\vartheta}) u_{\tilde{a}}}{a - \underline{a}^{\vartheta}} & \underline{a}^{\vartheta} \le x < a \\ u_{\tilde{a}} & x = a \\ \frac{x - a + (\overline{a}^{\vartheta} - x) u_{\tilde{a}}}{\overline{a}^{\vartheta} - a} & a < x \le \overline{a}^{\vartheta} \\ 1 & othrewise, \end{cases} \quad (3)$$

The values $w_{\tilde{a}}$ and $u_{\tilde{a}}$ respectively represent the maximum degree of the membership and the non-membership such that $w_{\tilde{a}}, u_{\tilde{a}} \in [0,1]$and $w_{\tilde{a}} + u_{\tilde{a}} \in [0,1]$. The same is depicted in Figure 1.

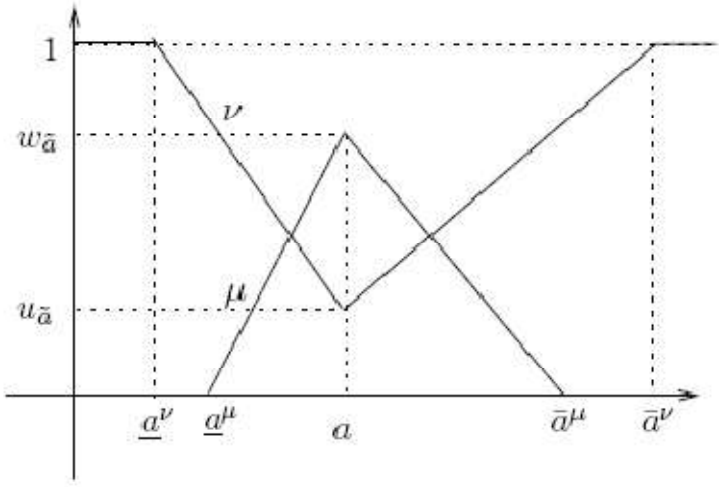

Figure 1: A membership and non-membership function in triangular intuitionistic fuzzy number

Definition 6; Let $\tilde{a} = \left\{\left(\underline{a}^{\mu}, a, \overline{a}^{\mu}; w_{\tilde{a}}\right), \left(\underline{a}^{\vartheta}, a, \overline{a}^{\vartheta}; u_{\tilde{a}}\right)\right\}$ and $\tilde{b} = \left\{\left(\underline{b}^{\mu}, b, \overline{b}^{\mu}; w_{\tilde{b}}\right), \left(\underline{b}^{\vartheta}, b, \overline{b}^{\vartheta}; u_{\tilde{b}}\right)\right\}$ be two TIFNs and k be a real number. Then

$$\tilde{a} + \tilde{b} = \left\{\left(\underline{a}^{\mu} + \underline{b}^{\mu}, a + b, \overline{a}^{\mu} + \overline{b}^{\mu}; \min\{w_{\tilde{a}}, w_{\tilde{b}}\}\right), \left(\underline{a}^{\vartheta} + \underline{b}^{\vartheta}, a + b, \overline{a}^{\vartheta} + \overline{b}^{\vartheta}; max\{u_{\tilde{a}}, u_{\tilde{a}}\}\right)\right\}.$$

ISSN (Online): 2305-0225
Issue 15(4), August 2014, pp. 469-475

$$k\tilde{a} = \begin{cases} \left\{\left(k\underline{a}^{\mu}, ka, k\overline{a}^{\mu}; w_{\tilde{a}}\right), \left(k\underline{a}^{\vartheta}, ka, k\overline{a}^{\vartheta}; u_{\tilde{a}}\right)\right\} & k > 0 \\ \left\{\left(k\overline{a}^{\mu}, ka, k\underline{a}^{\mu}; w_{\tilde{a}}\right), \left(k\overline{a}^{\vartheta}, ka, k\underline{a}^{\vartheta`}; u_{\tilde{a}}\right)\right\} & k < 0 \end{cases} \quad (4)$$

Definition 7; Let $\tilde{a} = \left\{\left(\underline{a}^{\mu}, a, \overline{a}^{\mu}; w_{\tilde{a}}\right), \left(\underline{a}^{\vartheta}, a, \overline{a}^{\vartheta}; u_{\tilde{a}}\right)\right\}$ be a TIFN. Then the value and the ambiguity of a$\tilde{a}$ are given as follows.

a) The value of the membership function of $\tilde{a}$ is

$$V_{\mu}(\tilde{a}) = \left(\underline{a}^{\mu} + 4a + \overline{a}^{\mu}\right)w_{\tilde{a}}/6$$

While the value of the non-membership function is

$$V_{\vartheta}(\tilde{a}) = \left(\underline{a}^{\vartheta} + 4a + \overline{a}^{\vartheta}\right)(1 - u_{\tilde{a}})/6$$

b) The ambiguity of the membership function of $\tilde{a}$ is

$$A_{\mu}(\tilde{a}) = \left(\overline{a}^{\mu} - \underline{a}^{\mu}\right)w_{\tilde{a}}/3$$

While the ambiguity of the non-membership function of $\tilde{a}$ is

$$A_{\vartheta}(\tilde{a}) = \left(\overline{a}^{\vartheta} - \underline{a}^{\vartheta}\right)(1 - u_{\tilde{a}})/3$$

Definition 8; Let $\tilde{a} = \left\{\left(\underline{a}^{\mu}, a, \overline{a}^{\mu}; w_{\tilde{a}}\right), \left(\underline{a}^{\vartheta}, a, \overline{a}^{\vartheta}; u_{\tilde{a}}\right)\right\}$ be a TIFN. Then the value index and the ambiguity index of $\tilde{a}$ are respectively defined as follows

$$V(\tilde{a}, \lambda) = V_{\mu}(\tilde{a}) + \lambda\left(V_{\vartheta}(\tilde{a}) - V_{\mu}(\tilde{a})\right)$$

And

$$A(\tilde{a}, \lambda) = A_{\vartheta}(\tilde{a}) - \lambda\left(A_{\vartheta}(\tilde{a}) - A_{\mu}(\tilde{a})\right)$$

Where $\lambda \in [0,1]$ is a weight represents the decision maker's (DM) preference information. It allows flexibility to incorporate the subjective attitude of DM in the model. $\lambda \in [0,0.5]$shows the pessimistic behavior while $\lambda \in [0.5,1]$ indicates optimistic behavior of the DM, and $\lambda = 0.5$ can be interpreted as an indifferent attitude of the DM.

Note that for any λ, $A(\tilde{a}, \lambda) \geq 0$. We say that a TIFN $\tilde{a}$ is non-negative if $V(\tilde{a}, \lambda) \geq 0$. Define

$F(\tilde{a}, \lambda) = V(\tilde{a}, \lambda) - A(\tilde{a}, \lambda)$

For a predefined value of $\lambda \in [0,1]$, Dubey and Mehra [8] define a new ranking relation for TIFNs $\tilde{a}$ and $\tilde{b}$ as follows

$\tilde{a} \leq \tilde{b}$if and only if $F(\tilde{a}, \lambda) \leq F(\tilde{b}, \lambda)$.

3. Proposed Model

3.1. Notations

d_i: The assigned duration d_i of activity i.

ES_i:The earliest time activity i can start once the previous dependent activities are over.

EF_i: The earliest time activity i is finished.

LS_i: It is equal to the latest finish time minus the time required to complete the activity.

LF_i: The latest time activity i can finish without delaying the project.

r_{ij}: Intensity of relation between activity i and activity j.

$P(j)$: A set of immediate predecessors of activity j.

$S(j)$: A set of immediate successors of activity j.

3.2. Algorithm Modules

The critical path method (CPM) is a step-by-step technique for process planning that defines critical and non-critical tasks with the goal of preventing time-frame problems and process bottlenecks. For the project network, we will actually be computing four basicfuzzy values for each node. Two of them, the ES early start times and the EF early finish times, are computed in a forward pass. The other two of them, the LF late finish times and the LS late start times, are computed in a second backward pass. The mentioned values are obtained by carrying out the calculations in the next modules.

3.2.1. Forward Pass Procedure

Consider the fuzzy project network (AON), where the duration time of each activity in a fuzzy project network is represented by TIFN. Forward pass is a technique used to determine the early start and early finish date for an activity. It involves moving forward through a network diagram to calculate the activity duration. Following steps describe the process:

Step F1: calculate ES_j using following calculation:

$$ES_j = \left\{\left(ES_{j_1}^{\mu}, ES_{j_2}, ES_{j_3}^{\mu}; w_{ES_j}\right), \left(ES_{j_1}^{\vartheta}, ES_{j_2}, ES_{j_3}^{\vartheta}; u_{ES_j}\right)\right\} = MAX\left\{r_{ij}(ES_i + d_i)\right\}_{i \in P(j), P(j) \neq \emptyset} \quad (5)$$

In above, r_{ij} assigns linguistic terms shown in Table 1 as preference relations between Activity i and Activity j.

ISSN (Online): 2305-0225
Issue 15(4), August 2014, pp. 469-475

Table 1
Nine-point intensity of relation scale and its description

Linguistic Terms	Intensity of relation
Equally relation	0.1
Moderately more relation	0.3
Strongly more relation	0.5
Very strongly more relation	0.7
Extremely more relation	0.9
Intermediate values	0.2, 0.4, 0.6, 0.8

MAX is calculated by the function F, which is described in Definition 8. For convenience, $\lambda = 0.5$which is interpreted as an indifferent attitude of decision maker.

Step F2: calculateEF_j using following calculation:

$$EF_j = ES_j + d_j \tag{6}$$

Note: for start time of the project we can suppose $ES_s = \{(s_1^{\mu}, s_2, s_3^{\mu}; w_s), (s_1^{\vartheta}, s_2, s_3^{\vartheta}; u_s)\}$.

3.2.2. Backward Pass Procedure

The Backward Pass is used to determine the Latest Time for each activity. The latest start time represents the latest time an activity can begin without delaying a project. To perform a Backward Pass, begin at the end of the project and move backward. Following steps describe the process:

*Step B0:*the fundamental manner of the backward pass is based on an inversion between addition and subtraction that is faces serious problems; negative time and violation of convex condition [7]. Following flow propose a subtraction operation that doesn't face with mentioned problems.
Suppose $a = \{(a_1^{\mu}, a_2, a_3^{\mu}; w_a), (a_1^{\vartheta}, a_2, a_3^{\vartheta}; u_a)\}$ and $b = \{(b_1^{\mu}, b_2, b_3^{\mu}; w_b), (b_1^{\vartheta}, b_2, b_3^{\vartheta}; u_b)\}$ are two TIFNs. We have to found $a - b$ subtraction. If c be defined as $a - b = c$ and $c = \{(c_1^{\mu}, c_2, c_3^{\mu}; w_c), (c_1^{\vartheta}, c_2, c_3^{\vartheta}; u_c)\}$ then

$$c_1^{\mu} = Max\{0, a_1^{\mu} - b_1^{\mu}\} \quad c_1^{\vartheta} = Max\{0, a_1^{\vartheta} - b_1^{\vartheta}\}$$
$$c_2 = Max\{0, a_2 - b_2\} \quad c_3^{\vartheta} = Max\{0, a_3^{\vartheta} - b_3^{\vartheta}\}$$
$$c_3^{\mu} = Max\{0, a_3^{\mu} - b_3^{\mu}\} \quad u_c = Max\{u_a, u_b\}$$
$$w_c = Min\{w_a, w_b\} \tag{7}$$

Using this relations lead to a full positive time. Also, following rules update attained TIFN and the problem due to the appearance of the non-convex time is resolved.

Rule 1: If $c_3^{\mu} < c_2$ then $c_2 = c_3^{\mu}$
Rule 2: If $c_2 < c_1^{\mu}$ then $c_1^{\mu} = c_2$
Rule 3: If $c_3^{\vartheta} < c_2$ then $c_2 = c_3^{\vartheta}$
Rule 4: If $c_2 < c_1^{\vartheta}$ then $c_1^{\vartheta} = c_2$ (8)

Step B1: calculate LF_j using following calculation:

$$LF_i = \{(LF_{i_1}^{\mu}, LF_{i_2}, LF_{i_3}^{\mu}; w_{LF_i}), (LF_{i_1}^{\vartheta}, LF_{i_2}, LF_{i_3}^{\vartheta}; u_{LF_i})\} = MIN\{r_{ij}(LF_j - d_j)\}_{j \in S(j), S(j) \neq \emptyset} \tag{9}$$

MIN is calculated by the function F, which is described in Definition 8. For convenience, $\lambda = 0.5$which is interpreted as an indifferent attitude of decision maker.

Step B2: calculateLS_j using following calculation:

$$LS_j = LF_j - d_j \tag{10}$$

Note: for finish time of the project we can suppose $EF_f = LF_f$.

4. Numerical Example

In order to prove the feasibility and superiority of our new method, we give an application example as follows.

Suppose that Fig.2 shows the network representation of a fuzzy project network.

ISSN (Online): 2305-0225
Issue 15(4), August 2014, pp. 469-475

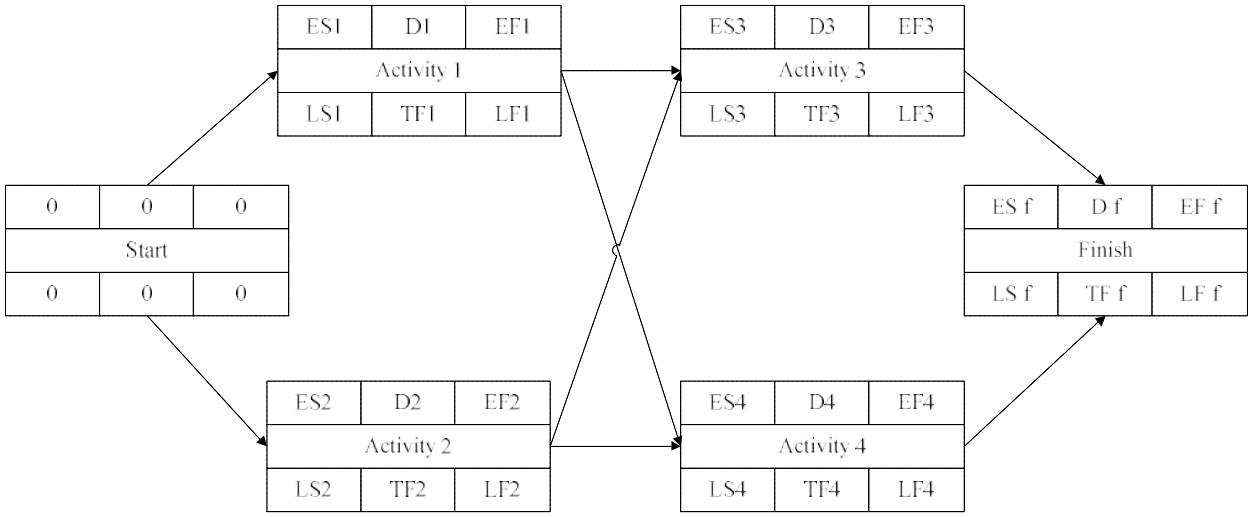

Figure 2: Fuzzy network of numerical example.

Also, Table 2 introduces the duration of activities are TIFNs and their relations intensity. With regard to proposed method, calculation of network characteristics is done as follows.

Table 2
Characteristics of fuzzy network

Activity	Duration (TIFNs)	Successor	Predecessor	Relation Intensity
Start (0)	0	1, 2	-	$r_{01} = 0.9, r_{02} = 0.7$
1	{(2,4,5,0.5),(1,4,5,0.1)}	3, 4	Start	$r_{13} = 0.6, r_{14} = 0.3$
2	{(4,7,9,0.9),(3,7,10,0.1)}	3, 4	Start	$r_{23} = 0.9, r_{24} = 0.5$
3	{(5,8,9,0.8),(2,8,10,0.2)}	Finish	1, 2	$r_{3f} = 0.9$
4	{(1,5,5,0.7),(1,5,6,0.2)}	Finish	1, 2	$r_{4f} = 0.9$
Finish (f)	0	-	3, 4	-

Our aim is to determine the ES, LS, EF and LF for all activities with regard to mentioned data in Table 2.

(a) Applying forward pass procedure according to the calculation of *Step F1* and *Step F2*, we can summarize acquired result in following table:

Table 3
Forward Pass calculations

Activity	Earliest Start	Earliest Finish	Precedence's Ranking
1	{0}	{(2,4,5,0.5),(1,4,5,0.1)}	No Ranking
2	{0}	{(4,7,9,0.9),(3,7,10,0.1)}	No Ranking
3	{(3.6,6.3,8.1,0.9),(2.7,6.3,9,0.1)}	{(8.6,14.3,17.1,0.8),(4.7,14.3,19,0.2)}	$F(0.9EF_2,0.5)>F(0.6EF_1,0.5)$
4	{(2,3.5,4.5,0.9),(1.5,3.5,5,0.1)}	{(3,8.5,9.5,0.7),(2.5,8.5,11,0.2)}	$F(0.5EF_2,0.5)>F(0.3EF_1,0.5)$
finish	{(7.74,12.87,15.39,0.8),(4.23,1287,17.1,0.2)}	{(7.74,12.87,15.39,0.8),(4.23,1287,17.1,0.2)}	$F(0.9EF_3,0.5)>F(0.9EF_4,0.5)$

For example, forward pass's characteristics of *Activity 3* are calculated as following:

$ES_3 = MAX\{(0.6 * EF_1), (0.9 * EF_2)\} = ?$

$$F\big((0.6 * EF_1), (\lambda = 0.5)\big) = V - A$$
$$= \{1.15 + 0.5 * (1.98 - 1.15)\}$$
$$- \{0.72 - 0.5 * (0.72 - 0.3)\} = 1.055$$

ISSN (Online): 2305-0225
Issue 15(4), August 2014, pp. 469-475

$$\mathrm{F}\big((0.9 * \mathrm{EF}_2), (\lambda = 0.5)\big) = \mathrm{V} - \mathrm{A}$$
$$= \{5.535 + 0.5 * (5.53 - 5.53)\}$$
$$- \{1.89 - 0.5 * (1.89 - 1.35)\} = 3.915$$
$$\mathrm{F}\big((0.9 * \mathrm{EF}_2), (\lambda = 0.5)\big) > F\big((0.6 * \mathrm{EF}_1), (\lambda = 0.5)\big)$$
$$ES_3 = 0.9 * EF_2 = \{(3.6,6.3,8.1,0.9), (2.7,6.3,9,0.1)\}$$
$$EF_3 = ES_3 + d_3$$
$$= \{(8.6,14.3,17.1,0.8), (4.7,14.3,19,0.2)\}$$

(b) Applying proposed backward pass procedure according to the calculation of *Step B1* and *Step B2*, we can describe results in following table:

Table 4
Backward Pass calculations

Activity	Latest Finish	Latest Start	Successor's Ranking
4	{(6.97,11.58,13.85,0.8),(3.81,11.58,15.39,0.2)}	{(5.97,6.58,8.85,0.7),(2.81,6.58,9.39,0.2)}	No Ranking
3	{(6.97,11.58,13.85,0.8),(3.81,11.58,15.39,0.2)}	{(1.97,3.58,4.85,0.8),(1.81,3.58,5.39,0.2)}	No Ranking
2	{(2.98,3.29,4.43,0.7),(1.41,3.29,4.7,0.2)}	{0}	F(0.5LS$_4$,0.5)>F(0.9LS$_3$,0.5)
1	{(1.79,1.97,2.65,0.7),(0.84,1.97,2.82,0.2)}	{0}	F(0.3LS$_4$,0.5)>F(0.6LS$_3$,0.5)
Start	{0}	{0}	No Ranking

According to above calculations, it is performed ways of determining the early or late start (forward pass) or early or late finish (backward pass) for a network in uncertainty environment with regard to proposed algorithm.

5. Conclusion

In this paper, we attempted to solve project scheduling problem with absolute uncertainty of fuzziness. Intuitionistic fuzzy number was introduced and project scheduling problem with fuzzy activity duration times and relation between activities was dealt with. A holistic algorithm is designed and a numerical example was given to illustrate the effectiveness of the proposed algorithm.

6. References

[1] D. F. Li, Fuzzy multi-objective many-person decision makings and games, National Defense Industry Press, Beijing, 2003.
[2] X. Y. Su, Z. H. Zhao, H. J. Zhang, Z. Q. Li, Y. Deng, An integrative assessment of risk in agriculture system, Journal of Computational Information Systems, 7 (2011), 9 – 16.
[3]T. Bhaskar, (2005), On quality of scheduling for resource constrained project scheduling problem, Indian Institute of Management Calcutta (Thesis).
[4] L. A. Zadeh, Fuzzy sets, Information Control, 8 (1965), 338 – 356.
[5] K. T. Atanassov, Intuitionistic fuzzy sets, Fuzzy Sets and Systems, 20 (1986), 87 – 96.
[6] L. A. Zadeh, (1975) The concept of a linguistic variable and its application to approximate reasoning. Information Sciences 8: 199–249.
[7] A. Soltani, R. Haji, 2007. A Project Scheduling Method Based on Fuzzy Theory. Journal of Industrial and Systems Engineering, 1(1): 70-80.
[8] D. Dubey, A. Mehra. (2011), Linear programming with Triangular Intuitionistic Fuzzy Number, EUSFLAT Conference, 563-569.
[9] A.I. Slyeptosov, T.A. Tyshchuk,(2003). Fuzzy temporal characteristics of Operations for project management on the network models basis, European Journal of Operations Research, 147: 253 -265.
[10] P.Zielinski,(2005). On computing the latest starting times and floats of activities in anetwork with imprecise durations, Fuzzy Sets and Systems, 150: 53-76.
[11] Ravi Shankar,N., Sireesha,V., SrinivasaRao, K., Vani,N., (2010). Fuzzy Critical Path Method based on Metric Distance Ranking of Fuzzy Numbers, Int. Journal of Math. Analysis, 4(20):995-1006.
[12] Stefan Chanas and Jerzy Kamburowski,(1981). The use of fuzzy variables in PERT, Fuzzy sets and Systems, 5(1):11-19.
[13] I. Gazdik,(1983). Fuzzy Network Planning-FNET, IEEE transactions on reliability, R-32(3):304-313.
[14] Nasution S.H.(1994). Fuzzy Critical Path Method, IEEE transactions on Systems, Man and Cybernetics, 24:48-47.
[15] Lorterapong, P. And Moselhi, O.,(1996). Project-network scheduling using Fuzzy Set theory, Journal of construction engineering and management, ASCE, 122(4):308-318.
[16] McCahon, C.S.(1993). Using PERT as an approximation of fuzzy project network analysis, IEEE transactions on Engineering Management, 40(2):146-153.
[17] Chang, S., T.Sujimura,Y. and Tazawa, T.(1995). An efficient approach for large scale project planning based on

ISSN (Online): 2305-0225
Issue 15(4), August 2014, pp. 469-475

Fuzzy Delphi Method, Fuzzy Sets and Systems, 76:277-288.
[18] Lin, F.T., Yao, J.S. (2003). Fuzzy Critical Path Method based on signed distance ranking and statistical confidence- interval estimates, Journal of Super Computing, 24(3):305-325.
[19] Kuchta, D. (2001). Use of Fuzzy numbers in project risk (criticality) assessment, International Journal of Project Management, 19:305-310.
[20] Yao, J.S., Lin, F.T. (2000). Fuzzy Critical Path Method based on signed Distance Ranking of fuzzy numbers, IEEE transactions on Systems, Man and Cybernetics, 30(1):76-82.
[21] S.Chanas, P.Zielinski, (2001). Critical path analysis in the network with fuzzy activity times, Fuzzy sets and Systems 122: 195-204.
[22] Kaufmann A., Gupta M. (1985), Introduction to fuzzy arithmetic theory and applications; Van Nostrand Reinhold; New York.
[23] Nasution S.H. (1994), Fuzzy critical path method; IEEE Transactions on Systems, MAN, AND Cybernetics 41(1); 48-57.

ISSN (Online): 2305-0225
Issue 15(4), August 2014, pp. 476-481

Effect of nano Ag+Silica composite packaging on quality and storage life of fresh-cut fruit nectarin cv. "Red Gold"

Saveh Vaezi, Mohammad Reza Asghari and Ali Reza Farokhzad

***Abstract*— Effect nanocomposite-based packaging was prepared by blending polypropylene (PP) with nano-Ag, nano Silica on the quality attributes and postharvest life of the fresh-cut fruits nectarin(cv. Red Gold) during storage at 0-1 ^{0}C with 90-95% RH for 21 days was studied. Compared with the control (PP), nanopackaging significantly reduced the fruit decay and weight loss rate (p<0/01). polyphenoloxidase (PPO), peroxidase (POD) activities and Browning index were decreased in nanopackaging fruit. These results indicate that nano-Ag+ Silica active packaging could be a viable technique to reduce fruit decay and maintain quality in "Red Gold" fresh-cut nectarins during postharvest storage.**

***Keywords*— Fresh-cut "Red Gold" nectarin, nano-Ag + Silica packaging, quality**

I. INTRODUCTION

Fresh-cut fruits and vegetables are slightly processed products which are prepared with peeling and slicing with or without washing [1]. Due to this processing, storage life of these products usually decreases 1 to 3 days or more [2]. Using of commercial disinfectants, UV radiation, heat and chemical treatments and packaging can be useful for increasing the shelf life of these fresh cut products. But these methods reduce their marketability, freshness and nutritional quality [3]. Therefore, the active packaging can be effective to maintain the nutritional quality of fresh-cut products [3]. Using of nanotechnology in food packaging industry has provided practical solutions in conjunction with increasing the storage life of food [4]. Since the nanoparticles are dispersed in the polymer as multiple parallel layers, path of the gases within the polymer becomes longer. However, the films prepared from nanocomposites are impermeable and because of lower percentage of nanoparticles (maximum 5%) the sheet produced for packaging, does not lose their clarity [5]. Because of antimicrobial effects of silver nanoparticles against bacteria, viruses and other eukaryotic microorganisms, silver nanoparticles have the highest antimicrobial activity [6]. Silica nanoparticles have also anti-bacterial properties. There for it can be used in edible coatings [7]. In this study, due to the unique charactrestics of nanocomposites containing silver nanoparticles and silica such as antimicrobial and prevention against oxygen infiltration, effects of this type of packing on the quality and storage life of fresh cut nectarines were investigated.

Saveh Vaezi is with the Urmia University, Urmia, IRAN (corresponding author to provide phone: 09144321636; e-mail: (vaezisaveh@yahoo.com).

Mohammad Reza Asghari, was with Urmia University,Urmia, IRAN. He is now with the Department of Agriculture, Urmia University, (e-mail:m.asghari@urmia.ac.ir).

Ali Reza Farokhzad is with the Agriculture Department, University of Urmia, Urmia, IRAN,(e-mail: a.farokhzad@urmia.ac.ir).

II. MATERIALS AND METHODS

'Red Gold' nectarines harvested at commercial maturity stage from an orchard in Urmia (West Azerbaijan, Iran) were selected on the basis of uniformity in color, size and firmness. The fruits were disinfected by immersing in 200 L L^{-1} chlorine tank for 10 min, then washed with potable water and finally dried with absorbent paper. All cutting boards, utensils and containers were also sanitized with 200 L L^{-1}chlorine to minimize the microorganism pollution. The sanitized fruits were cut at the extremes with a knife and after slicing were packaged in nano Ag+Silica packaging and or in polyethylene bag without nano particle and stored at 0-1^{0}C for 21 days. The packages had bought from Nano Bespar Atick company.

A. Determination Decay Index

In each replicate 15 fruits were selected for determining the decay index. Fruits were putted in four classes according to decay extent: 0= no decay, 1= less than 30% of fruit were decayed, 2= between 30% - 70% of fruit were decayed and 3= more than 70% of fruit were decayed [8].

ISSN (Online): 2305-0225
Issue 15(4), August 2014, pp. 476-481

B. Determination of Weight Loss

After packaging, fresh cut nectarine were weighed at the beginning of the experiment and thereafter each 7 day during the storage period. Weight loss was expressed as the percentage loss of the initial total weight [9].

C. Measurement of Titrtable Acidity (TA) and Total Soluble Solid (TSS)

TA was determined by titration with 0.1 M NaoH to pH 8.2 and expressed as malic acid (mg) on the basis of fresh weight (FW) [10].

Fruit juice samples obtained randomly from berries in different parts of clusters. Total soluble solid of berry juice was determined by using a refractmeter (Atago, Japan) at 20 °C and the results were expressed as °Brix.

D. Browning Index

Browning index was determined according to the method described by [11] with a little modification. A colorimeter was used to measure the exterior color changes for the surface of nectarine slices. The color changes were quantified by the tristimulus colour values (L^* , a^* and b^*)

BI = 100 (x – 0/3) / 0/1752 , where x = (a + 1/79 L^*) / (5.645 L^* + a^* - 3. 072 b^*).

E. Determination of Polyphenol Oxidase (PPO) and Peroxidase (POD) Activity

PPO activity was assayed with 4-methylcatechol as a substrate according to the method of [12]. Assay of PPO activity was performed using 1 ml of 0.1 M phosphate buffer (pH 6.4), 0.5 ml of 0.1 m 4- methylcatecld and 0.5 ml enzyme solution. The increase in absorbance at 420 nm at 25^0c was automatically recorded for 3 min. One unit of enzyme activity was defined as the amount which caused a change of 0.01 in absorbance per minute.

Peroxidase activity was assayed according to the method by [13]. The reaction mixture (4.6 ml) contained 2.5 ml of 0.05 M phosphate buffer (pH=7), 1 ml of 1% guaiacum (w/v), 0.1 ml of enzyme extract and 1 ml of 1% H_2O_2 (v/v). One unit of POD enzyme activity was defined as the amount that caused a change of 0.01 in the absorbance at 490 nm min^{-1}.

F. Statistical Analysis

All experiments data were analyzed using analysis of variance (ANOVA) with SAS (version 9.2) statistical software. Duncan's multiple range test was used to determine the difference of means, and $P<0.05$ was considered to be statistically significant, $P<0.01$ was considered to be highly significant.

III. RESULTS AND DISCUSSION

A. Determination Decay Index

The results showed that nanocomposite packaging containing silver and silicate, reduced the rate of decay during storage of fresh -cut nectarines (Fig. 1). Interaction effect container type and storage time on the amount of fruit decay was significantly in 1% level (Table I). Oxygen is problematical factor in the food package because this element spoilage the fat of food and change their color [14]. Nanoparticles had been inserted as stripe form in the new packaging films and such as barrier prevent the penetration of oxygen. In the other words, path of the gases within the polymer becomes longer and the freshness of food is better preserved [14]. Polyethylene plastic containing 0.1 to 0.8 wt % of silver nanoparticles, preserved storage life of dark green color vegetables (such as onion, spinach and coriander), which is easily destroyed, a week to a month more than ordinary plastics packaging [15]. Silver inherently has antibacterial and antifungal characteristics. With using of these containers compared with ordinary vessels in the first 24 hours of storage, bacterial growth rate decreased up to 98 % [6].

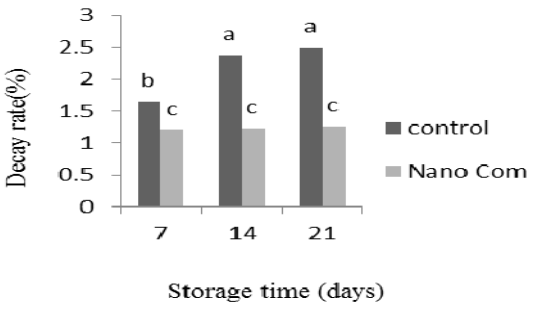

Fig.1 - Effect of nano Ag ,nano Ag+Silica packaging and normal packaging on decay rate of fresh-cut 'Red Gold' nectarine during 0-1°C storage

ISSN (Online): 2305-0225
Issue 15(4), August 2014, pp. 476-481

Table I. Table of variance analysis of postharvest treatments with different containers, time and their mutual effect on quality characteristics of fresh-cut 'Red Gold' nectarine during storage at temperature of 0-1 0C. * and ** respectively show the significant at probability level 5% and significant at probability level 1%

Source of variation	DF	Mean square Decay rate(%)	Weight loss rate(%)	TA(g/100 ml acid malic)
Container(z)	1	5/30**	0/026**	0/035**
Time(T)	2	0/48**	0/013**	0/069**
Container*Time(Z*T)	2	0/37**	0/001**	0/011*
Error	18	0/0044	0/00017	0/0026
Coefficient of variation(%)		3/91	8/92	6/81

B. Fruit Weight Loss

There is significant difference between polypropylene packages containing silver and silica nanoparticles and storage time and their interactions effects on the fruit weight loss was significantly in 1% level (Table I). In general, fruit weight loss in 21 days of maintenance in second type of package was dropped . Although weight loss was less in the packaging containing silver and silica nanoparticles (Fig. 2). Fruit weight loss is mainly associated with respiration and evaporation of moisture on the skin of fruits [16]. Dehydration and water loss from the fruit surface also result in weight loss fruit [16]. This result indicated that the nano-packing had a greater effect in preventing weight loss of fruit, which could be attributed to its better barrier properties against H_2O [17]. Kiwifruit package insert polymer nano-loss less weight than a conventional package within 42 days of storage [18]. These results agree with those reported by [19] and [18] on fresh-cut 'fuji' apple and kiwifruit packaged under coating of nano-ZnO , nano-Ag and nano TiO_2.

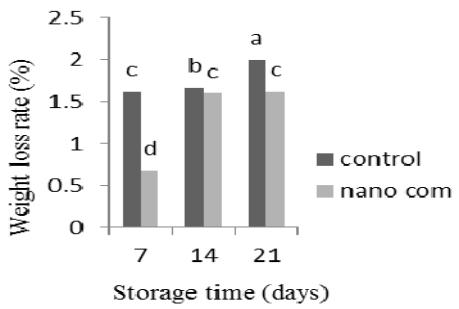

Fig. 2- Effect of nano Ag ,nano Ag+Silica packaging and normal packaging on Weight loss rate of fresh-cut 'Red Gold' nectarine during 0-1°C storage

C. Measurement of Titratable Acid and Total Soluble Solid

The effect of container type (silver and silica nanoparticles) and storage time at the 1 % level and their interaction effects at the 5 % was significant on titrtable acids (Table I). Titratable acids decreased during the 21 days, but in the fruits packaged in nano packaging showed less decline (Fig. 3). Based on the analysis of variance table II there is significant difference between nano packaging and storage time on the amount of soluble solids during storage . The maximum amount of TSS after 21 days were packaged polypropylene (Fig.4). Factors that reduced respiration and ethylene production, due to lower comsumption of sugars prevented of reduced organic acids and increased total soluble solid [20]. For jujubes, the nanopackaging was more effective at maintaining the content of TA than the control bags[17]. polyethylene packages containing silver nanoparticles compared to normal packages beneficial effect on physical, chemical and sensory Chinese jujube has been shown [17]. These results indicated that the application of nano-packing might be able to slow the metabolism to give prolonged storage life to the fruit. Reference [21] demonstrated that in strawberry fruits packaged in nano-silver containers titratable acids would go through less reduction. Reference [19]-[18] showed that nano-packaging have preserved more titratable acid rate in fresh-cut 'fuji' apple and kiwifruit compared to normal packaging.

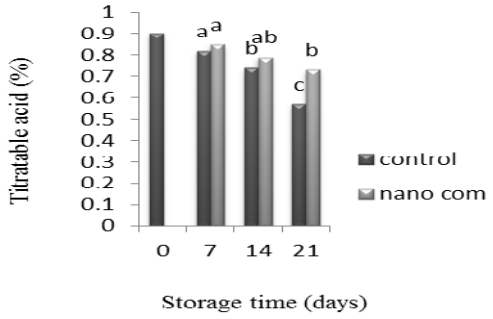

Fig.3- Effect of nano Ag ,nano Ag+Silica packaging and normal packaging on titratable acid of fresh-cut 'Red Gold' nectarine during 0-1°C storage

ISSN (Online): 2305-0225
Issue 15(4), August 2014, pp. 476-481

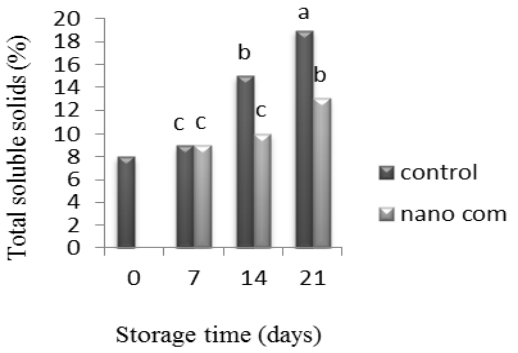

Fig. 4- Effect of nano Ag ,nano Ag+Silica packaging and normal packaging on total soluble solids of fresh-cut 'Red Gold' nectarine during 0-1°C storage

Table II. Table of variance analysis of postharvest treatments with different containers, time and their mutual effect on quality characteristics of fresh-cut 'Red Gold' nectarine during storage at temperature of 0-1 0C. * and ** respectively show the significant at probability level 5% and significant at probability level 1%

	Mean square		
Source of variation	DF	TSS (%)	BI
Container(z)	1	0.082**	601.80**
Time(T)	2	0.068**	222.18**
Container×Time(Z×T)	2	0.021**	29.19**
Error	18	0.0017	0.044
Coefficient of variation(%)		8.35	0.33

D. Browning Index(BI)

The lowest browning polypropylene packages containing silver nanoparticles and silica were recorded after 7 days (Fig. 5). significant difference between polypropylene packages containing silver and silica nanoparticles and their interactions effects was significantly in 1% level (Table II). Cutting and destruction of the cells at the cut surface , the color change occurs . When the cells are broken oxidase and precursor are in contact with each other , that is leading to oxidation and enzymatic browning [22] . These results agree with those reported by [23] on fresh-cut asparagus spears slices packaged under coating of silver nanoparticles- PVP. Low-O_2 and high-CO_2 condition can decrease fruit surface browning. This reduction in the browning is associated with some physiological effects such as a decrease in respiration rates and a delay in the climacteric onset of the rise in ethylene [24]. For jujubes, the nano packaging was more effective at decrease browning index than the control bags [17]. browning rate reduced in fresh orange juice packaged under nano Ag and nano-ZnO-coated active packaging compared with normal packaging [4]- [19].

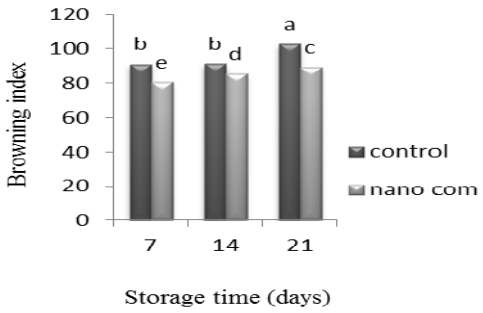

Fig. 5- Effect of nano Ag ,nano Ag+Silica packaging and normal packaging on browning index fresh-cut 'Red Gold' nectarine during 0-1°C storage.

E. Determination of polyphenol oxidase (PPO) and peroxidase (POD) activities

Polyphenol oxidase and peroxidase activites increased in the past 21 days on all packaging but in polypropylene packages containing silver and silica nanoparticles, the amount of enzymes activity of polyphenol oxidase and peroxidase lower compared with conventional polymer containers (Fig. 6,7). Interaction effects container type and storage time on the amount of enzyme activity of polyphenol oxidase was significantly in 1% level and Interaction effects container type and storage time on the amount of enzyme activity of peroxidase was significantly in 5% level (Table III). Oxidative browning usually occurs when the enzyme polyphenol oxidase in the presence of oxygen phenolic compounds in fruits and vegetables changes to the dark pigments [25] . POD is another oxidoreductase enzyme involved in enzymatic browning since diphenols may function as reducing substrates in its reaction [26]. Peroxidases are widely distributed in the plant kingdom and have been shown to participate in different physiological processes like lignifications and wound healing [27]. References [28] reported a role for POD in damaged tissues, describing its participation in the cross-linking of the cell wall and in tissues infected with pathogens. Reference [18] showed that polyphenols oxidize activity in nano-composite packages or oxidation amount of polyphenols by these enzymes decrease significantly in fruits placed in nano containers. In previous work, the inhibitory effect of nanopackaging on PPO and POD activitise was also found in strawberry fruit [21]. For fresh-cut 'fuji' apple the nano packaging was more effective

ISSN (Online): 2305-0225
Issue 15(4), August 2014, pp. 476-481

at reduced PPO and POD activitise than the normal packaging [19].

Table III. Table of variance analysis of post-harvest treatments with different containers, time and their mutual effect on quality characteristics of fresh-cut 'Red Gold' nectarine during storage at temperature of 0-1 0C. * and ** respectively show the significant at probability level 5% and significant at probability level 1%

	Mean square		
Source of variation	DF	PPO(U/g/min)	POD(U/g/min)
Container(z)	1	1188**	865/58**
Time(T)	2	4876**	113/17**
Container×Time(Z×T)	2	6755**	194/88*
Error	18	9883/3	401/40
Coefficient of variation(%)		13/86	32/48

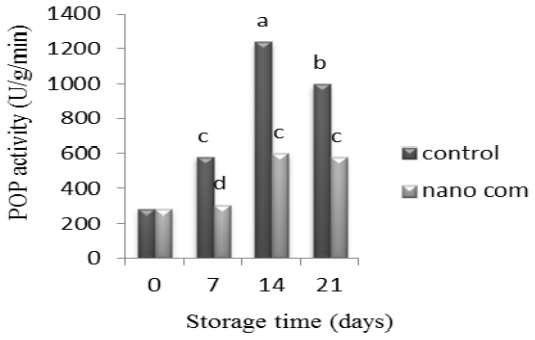

Fig. 6- Effect of nano Ag ,nano Ag+Silica packaging and normal packaging on polyphenol oxidase of activitiy fresh-cut 'Red Gold' nectarine during 0-1°C storage.

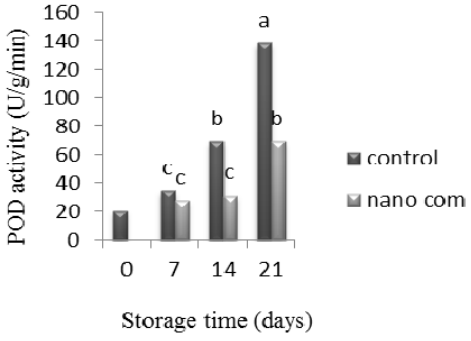

Fig. 7- Effect of nano Ag ,nano Ag+Silica packaging and normal packaging on peroxidase of activitiy fresh-cut 'Red Gold' nectarine during 0-1°C storage.

IV. CONCLUSIONS

A novel nano Ag+Silica packaging film were successfully applied to the preservation of fresh-cut 'Red Gold' nectarine during 0-1°C storage for 21 days. The results showed that nano Ag+Silica coating were more beneficial in keeping the preservation quality of fresh-cut products than the normal packaging. Coating of nano composite reduced weight loss rate, maintained TA levels, inhibited the activity of PPO and POD.

REFERENCE

[1] FDA, "FDA Fact Sheet: Fresh-cut fruits and vegetables. Draft Final Guidance" *FDA PressOffice*., vol. 301, pp. 827-6242, Apr. 2007.

[2] A. Allende, F. A. Tomas-Barberan, and M. I. Gil, "Minimal processing for healthy traditional foods" *Trends Food Sci Technol*., vol. 17, pp. 513–519, May. 2006.

[3] G. A. Conzalez_Aguilar, E. Valenzuela_soto, J. Lizardi _ Meudoza, and F. F. Ayalazavala, "Effect of chitosan coatiny in preventing deterioration and preserving the quality of fresh - cut papaya" *J of Sci of Food Agri*., vol. 89, pp. 15-23, Aug. 2010.

[4] A. Emami Far, M. Kadivar, P. Solaimni, 2011. "Evaluation of nano composite package in gcontaining nano-silver and nano zinc oxideon Lnbar deeplove fresh orange juice" *J of Food Tech*., vol. 1, pp. 57-67, Sep. 2011.

[5] S. Hotta1, and D. R. Paul, "Nanocomposites formed from linear low density polyethylene and organoclays" *J of Polym Sci*., vol. 45, pp. 7639-7642, Aug. 2004.

[6] A. Brody, and B. Bugusu, "Lnnovative food packaging solutions" *J of Food Sci*., vol. 73, pp. 107-116, Sep. 2008.

[7] A. Fujishima, T. N. Rao, and D. A. Tryk, "Titanium dioxide photocatalysis" *J photochem photobiol C*., vol. 1, pp.1-21, Nov. 2000.

[8] S. H. Zhu, J. Zhou, "Effect of nitric oxide on ethylene production in strawberry fruit during storage" *J Food Chem*., vol. 100, pp. 1517-1522, Feb. 2007.

[9] X. Meng, J. LiBLiu, and S. Tian, "Physiological responses and quality attributes of table grape fruit to chitosan preharvest spray and postharvest coating during storage," *J Food Chem.*, vol.106, pp. 501-508, Mar. 2007.

[10] P. Hernandez-Munoz, E. Almena, V. D. Valle, D. Velez, and R. Gavara, "Effect of chitosan coating combine with postharvest calcium treatment on strawberry (Fragaria ananassa) quality during refrigerate storage" *J Food Chem*., vol. 110, pp. 428-435, May. 2008.

[11] M. P. Buera, R. D. Lozano, and C. Petriella, "Definition of colour in the non enzymatic browning process," *Die Farbe*., vol. 32, pp. 318–322, Nov. 1985.

[12] F. Pizzocaro, D. Torreggiani, and G. Gilardi "Inhibition of apple polyphenoloxidase (PPO) by ascorbic acid, citric acid and sodium chloride," *J Food Proces Preser*., vol. 17, pp.21-30, Apr.1993.

[13] A. Updhyaya, D. Sankhla, T. D. Davis, N. Sankhla, and B. N. Smidth, "Effect of paclobutrazol on the activities of some enzymes of activated oxygen metabolism and lipid peroxidation in senescing soybean leaves. *J Plant Phys.*, vol. 121, pp. 453-461, Feb. 1985.

[14] D. R. Paul, and L. M. Robeson, "Polymer nanotechnology" *J Polymer*., vol. 49, pp. 3187-3204, June. 2008.

[15] K. F. Chang, and P. C. Chou, " A study on the psychology satisfaction influenced by the indoor physical environment factors-taking the thermal comfort factor" *J Food Chem*., vol. 18, pp. 7-6, Oct. 2007.

ISSN (Online): 2305-0225
Issue 15(4), August 2014, pp. 476-481

[16] D. N. Martínez-Romero, J. M. Alburquerqu, F. Valverde, S. Guillén, D. Castillo, and M. Valero, "Postharvest sweet cherry quality and safety maintenance by *Aloe vera* treatment: a new edible coating," *Postharvest Biol Tech*., vol. 39, pp. 93-100, May. 2006.

[17] H. M. Li, F. Li, and L. Wang, "Effect of nano-packaging on preservation quality of Chinese jujube (Ziziphusjujuba Mill. varinermis (Bunge) Rehd)," *J Food Chem*., vol.114, pp. 547–552, Sep. 2009.

[18] Q. Hu, Y. Fang, Y. Yang, N. Ma, and L. Zhao, "Effect of nanocomposite-based packaging on postharvest quality of ethylene-treated kiwifruit (Actinidia deliciosa) during cold storage" *Food Rese Inter*., vol. 44, pp. 1589-1596, Sep. 2011.

[19] W. Li, and Y. Li, "Effect of nano-ZnO-coated active packaging on quality of fresh-cut "fugi"apple," *J Food Scie Tech.*, vol. 46, pp.1947-1955, May. 2011.

[20] H. Hu, X. Li, Ch. Dong, and W. Chen, "Effects of wax treatment on quality and postharvest physiology of pineapple fruit in cold storage" *A J Biotech*., vol. 10, pp. 7592-7603, Apr. 2011.

[21] F. Yang, H. Li, F. Li, and Q. Hu, "Effect of nano-packaging on preservation quality of fresh Strawberry (*Fragaria ananassa* Duch.cv.Fengxiang) during storage at 4^0c," *J Food Sci*., vol. 75, pp. c236-c240, July. 2010.

[22] L. Vamos-Vigyazo, "Polyphenol oxidase in fruits and vegetables". *CRC. Food Sci Nut*., vol. 15, pp. 49-127, Oct. 1982.

[23] J. S. An, M. Zhang, S. J. Wang, and J. M. Tang, "Physical, chemical and microbiological changes in stored green asparagus spears as affected by coating of silver nano particles PVP," *LWT-Food Sci Tech*., vol. 41, pp. 1100–1107, Jun. 2008.

[24] T. Solomos, "Principles underlying modified atmosphere packaging. In: Minimally Processed Refrigerated Fruits and Vegetables " *J Food Chem*., vol.10, pp. 183–225, Apr. 1997.

[25] R. Baeza, "Comparison of thechnologiesto conyrol the physiologica, biochemical and nutritional changes of fresh-cut fruit" *Food Sci Gradu Prog*., vol. 10, pp. 109-115, Mar. 2007

[26] M. Chisari, R. N. Barbagallo, and G. Spagna, "Characterization of polyphenol oxidase and peroxidase and influence on browning of cold stored strawberry fruit," *J Agri Food Chem*., vol. 55, pp. 3469–3476, Feb. 2007.

[27] K. Wakamatsu, and U. Takahama, " Changes in peroxidase activity and in peroxidase isozymes in carrot callus" *Physio Plant*., vol. 88, pp. 167–171, Aug. 1993.

[28] C. L. Biles, and R. D. Martin, "Peroxidase, polyphenoloxidase, and shikimate dehydrogenase isozymes in relation to tissue type, maturity and pathogen induction of watermelon seedlings" *Plant Physi and Biochem*., vol. 31, pp. 499–506, May. 1993.

ISSN (Online): 2305-0225
Issue 15(4), August 2014, pp. 482-487

Numerical Simulation of Flow Field around a Darrieus Vertical axis wind turbine to Estimate Rotational wakes Size

Milad Babadi Soultanzadeh[1], Babak Mehmandoust Isfahani[2], and Davoud Toghrai Semiromi[3]

1)Ms Student, Mechanical Engineering Department, Islamic Azad University, Khomeini Shahr Branch. milad.babadi@iaukhsh.ac.ir
2)Assistance Prof, Mechanical Engineering Department, Islamic Azad University, Khomeini Shahr Branch. mehmandoust@iaukhsh.ac.ir
3) Assistance Prof, Mechanical Engineering Department, Islamic Azad University, Khomeini Shahr Branch. toghraee@iaukhsh.ac.ir

***Abstract*:** Due to the increasing energy cost and reducing fossil resources, also with respect to environmental pollutions, sustainable energy usage is inevitable. In the last decades wind power is allocated to a particular share of sustainable energies. Design and optimization of wind systems requires aerodynamics analysis. Computational fluid dynamics is a guaranteed method for aerodynamics analysis of wind turbines. In this work at first we introduce briefly Darrieus vertical axis wind turbines and discussed their advantages and disadvantages compared to the horizontal axis wind turbines. Then tried to use a computational fluid dynamics method to simulate flow field around the Darrieus vertical axis wind turbine with three straight blades that use NACA0016 airfoil as profile of blades. To do this, we used RNG K-ε turbulence model to solve RANS equations of fluid motion. Simulation has been performed for three values of the rotational speeds. Velocity distribution of wakes is obtained in some horizontal directions.

***Keywords*:** Computational Fluid Dynamics, Darrieus Wind Turbine, Sustainable Energy, Wind Energy, Vertical axis wind turbine.

I. INTRODUCTION

With increasing concerns about the environment, research on environmentally friendly renewable energy sources has increased. Focusing on these resources is due to increased environmental pollution (chemical and thermal pollution), increasing global demand for energy and reducing fossil energy resources. Renewable energy includes solar, biomass, geothermal, hydroelectric and wind energy. Wind energy is one of the most important that have put a various choices in front of researchers. This energy currently has the fastest growth rate among the other renewable resources.

Devices that are used for obtaining wind energy are known as wind turbines. A wind turbine is a device that converts the kinetic energy of wind into rotational energy of the rotor shaft [5]. They include two main groups, horizontal axis and vertical axis turbines. Vertical axis wind turbines are the first devices to convert wind energy to rational energy of shaft. Types of vertical axis turbine configurations include Darrieus, Savonius, Zephyr and windmills of Sistan [4].

Darrieus turbines have been installed at the first time in 1931. There are various configurations for Darrieus turbine blades that can be include straight-blade models, complex spiral curved blades and troposkein curved blades. Number of blades can vary from one to five (depending on economic considerations) [5]. Darrieus vertical axis wind turbines are the most efficient among the vertical axis wind turbines, but the main problems of them are low torque in starting and the lack of structural integrity [4].

Also the pitch angle of the blades can be fixed or variable. Changing the blade pitch angle can increase the torque to help better starting. Fixed pitch blades have a simpler structure, but produces less torque [4].

Currently, large scale vertical axis wind turbines is economically less attractive, but they can be used for areas far from the grid and Areas that are not suitable for wind farms of horizontal axis wind turbines. For this reasons, small scale vertical axis wind turbines have become more common in the world.

The main problems of vertical axis turbine are low start torque, rotor lift force, low efficiency and integrated structure. Instead, advantages compared to horizontal axis turbines are

ISSN (Online): 2305-0225
Issue 15(4), August 2014, pp. 482-487

as follows

• Not sensitive to the wind direction.

• The vertical axis blades have extra life because of the force of gravity and inertia is constant.

• Manufacturing costs are lower compared to the horizontal axis.

• Less sensitive to crossover turbulent flow and mechanical ability to work under storms and hurricanes conditions as they are safe.

• Due to the lower rotational speed than a horizontal axis turbine, vertical axis wind turbines are more silent [2], [5].

For this reasons, small vertical axis turbines can be installed close to the ground, on the roofs of houses in urban and rural environments and anywhere that turbulence is higher than wind farms sites.

Progression in the technology of vertical axis wind turbines need to increase the coefficient of performance, ability to start better, optimize the aerodynamic characteristics of airfoil used, study effects of solidity and blade pitch angle.

Fig. 1 illustrates average wind speed at a height of 40 m above ground level in different regions of Iran. Areas highlighted in red, light red and orange are suitable for wind farms of the horizontal axis wind turbines. Vertical axis turbines can be used in areas where wind speeds are lower and covered more area of the map.

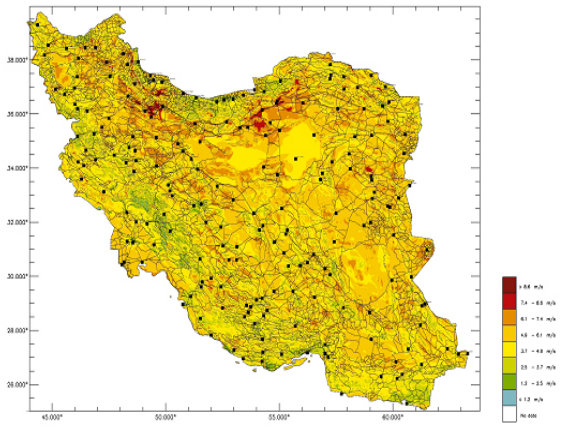

Fig.1 Mean wind velocity at height 40m (Iran)[]

Howell et al. [2] studied a small scale Darrieus vertical axis wind turbine both experimentally and numerically with computational fluid dynamics methods. They have tried to determine impact of some important parameters like wind speed, solidity and tip speed ratio on the turbine that used NACA0022 airfoils. Castelli et al. [3] applied a computational fluid dynamics method to a straight blade Darrieus turbine with tree blades to estimate the impact of aerodynamically loads and performance coefficient. Bhutta et al. [4] Reviewed researches on vertical axis wind turbines. Cao et al. [1] investigated the effect of rotational speed on the aerodynamic performance of vertical axis turbines. Li et al. [5] applied 2.5D and 3D computational fluid dynamics simulation using both the RANS equations and large eddy simulation to a vertical axis wind turbine.

The present paper aims to establish a better understanding of the aerodynamics of Darrieus vertical axis wind turbines and introduce a method to simulate the flow of this equipment by the computational fluid dynamics and RNG K-ε turbulence model. To do this, a Darrieus vertical axis wind turbine with three straight blades considered. Four digit symmetric NACA0016 airfoil are used and two-dimensional flow field is solved using a moving reference frame to consider rotational effect of the rotor.

II. DARRIEUS WIND TURBINE AERODYNAMICS

Solidity is one of the basic parameters of the Darrieus wind turbines. This parameter controls the rotational speed of the turbine to achieve maximum performance. High solidity usually lead to low tip speed ratio, which is one of another main parameters that cause reduced turbines performance coefficient. The high blade tip speed ratio provides a stronger interaction with the upstream wakes [2].

Both rigidity and tip speed ratio are dimensionless ratios, respectively, the equations (1) and (2) are introduced them.

$$\sigma = \frac{NC}{R} \tag{1}$$

$$\lambda = \frac{\omega R}{V_\infty} \tag{2}$$

In these equations N is the number of blades, C is chord length of blade (airfoil), R is the radius of the rotor, ω is the rotational speed of the rotor in radians per second and V_∞ is the free stream velocity. Fig. 2 illustrates the composition and shape of the Darrieus wind turbines. Fig. 3 shows the velocity triangles for the first blade when it rotates θ degree from reference condition. V is the absolute velocity of the fluid stream within the affected area by the rotation of the rotor. U is the linear velocity of the blade that is ωR and tangent to the circular path of the blade. W is the relative velocity to the blade. Blades are straight and NACA 0016 airfoil is used.

Air free stream moves toward the rotor, the rotor will absorb fraction of the kinetic energy of the air stream and leaving stream carry less energy than inflow (principle of conservation of energy). In other words, the wind turbines will act as a wind shade, obtained fraction of energy and a low-speed turbulent wake of air is formed in the back of turbine.

ISSN (Online): 2305-0225
Issue 15(4), August 2014, pp. 482-487

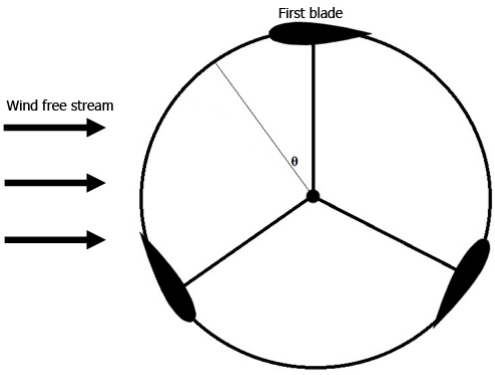

Fig. 2 Simulated Darrieus wind turbine with three blades configuration

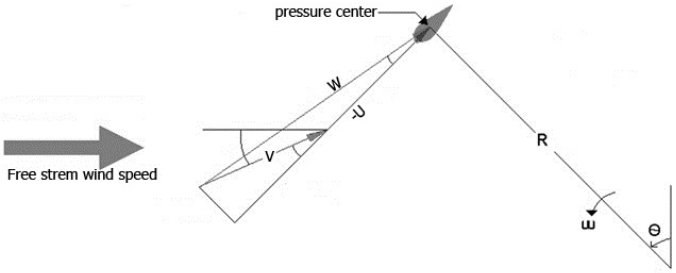

Fig. 3 Velocity triangles for first blade

III. NUMERICAL SIMULATION OF FLOW FIELD

To predict the behavior of wind turbines should be evaluated aerodynamic loads and flow field around turbines [4]. In fact, the complexity of three-dimensional vortex as well as dynamic stall should be considered. Experimental wind tunnel testing can help to better understand the aerodynamics of vertical axis wind turbines, but the cost of equipment and setups is really expensive. Also, results should be achieved in a manner that measuring devices have little effect on the flow field. These results should be modified to post-processing. Instead of experimental devices, computational fluid dynamics methods can provide details about the flow field without complex instruments usage. It also enables us to do regular studies like dimensional analysis without spending too much [5]. Although wind turbines work under unsteady three-dimensional flow but two-dimensional studies can be provide good results with an overview of the fundamentals [6]. Two-dimensional analysis disables to simulate tip vortex and usually examine rotor torque more than the maximum torque that experimental tests show.

Unlike horizontal axis wind turbines, vertical axis wind turbine is usually works under very high angles of attack conditions and the angle of attack is much more stalling angle. This phenomenon is more evident at low tip speed ratios. In the downstream areas (θ greater than 180 degrees), the blades are in the wake shadow region of the upstream blades, so finding the exact angle of attack of the blades is very difficult.

Stall occurs when the boundary layer flow is separated from the blade, in this case the lift force began to decline and rotational turbulent wakes are created. The blades in this area are under highly turbulent unsteady flow and non-linear behavior of the aerodynamic forces exerted on the blades. High turbulence in this region (wake shadow region) creates inaccuracy in calculating the downstream blade forces [5].

To simulate the flow field RNG K-ε turbulence model is used in this paper for solving the RANS equations. This model is derived using statistical methods and it's accurate for fast-strained flows. Also because of the consider swirl on the turbulence, it provides good results in vortex flows and turbomachinery flow modeling.

Fig. 4 illustrates flow field that solved. The rotor dimensions shown in this Figure is exaggerated because the domain size is much larger than rotor diameter. The grid near the rotor can be seeing in the Fig. 5. Finer grid near the rotor blades used to calculate field much more in line with reality results. Inaccuracy and errors in the grid production and the errors in the discrete equations of the flow controller equations play the role of free turbulence in computational fluid dynamics space.

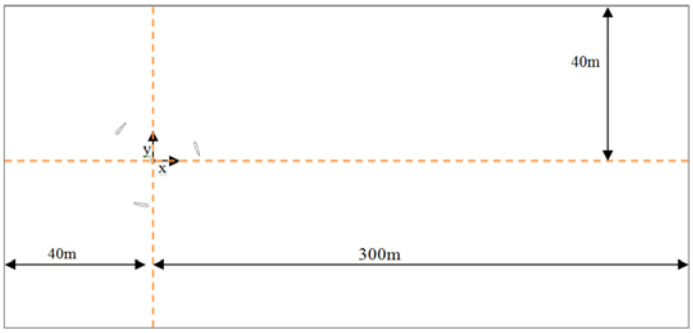

Fig. 4 Flow simulation Domain (with exaggerate)

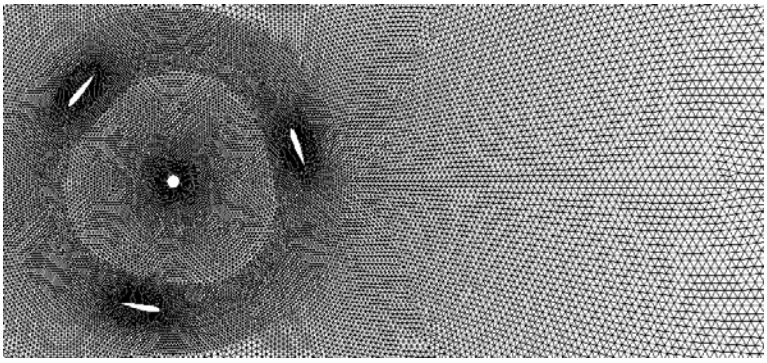

Fig. 5 Grids near the moving solid walls (near the rotor)

In turbomachineries due to rotational motion of the rotor

ISSN (Online): 2305-0225
Issue 15(4), August 2014, pp. 482-487

rotational flow is generated. It is better to use moving reference frame in this cases because the rotational motion of fluid is made because of the solid boundary rotation. This flow is inherently unsteady because rotor blades sweep a volume (surface in two-dimensional problems) of the environment but if there was not a stationary wall near the rotational boundary it's good to allocate a coordinate system to moving (rotational) frame and solved the problem as steady flow. In this new coordinate system grids rotate with frame (rotor) and there is not any relative velocity between blades and cells. Since Darrieus vertical axis wind turbine is a turbomachinery we could use this method to simulate the flow field. Fig. 6 illustrates the region that new frame has been attributed to it.

Once the simulation is done when rotor is in θ=45. In this case, flow domain is solved for the three rotational speed ω, respectively, 5, 8 and 12 rad/s. In each case the tip speed ratio λ is equal to 1.5, 2.4 and 3.6 respectively. In all cases free stream velocity consider V_∞=10m/s.

Note that in all cases the tip speed ratio is lower than 4, so turbine blades operate in conditions of high stall. Table (I) provide details of the rotor.

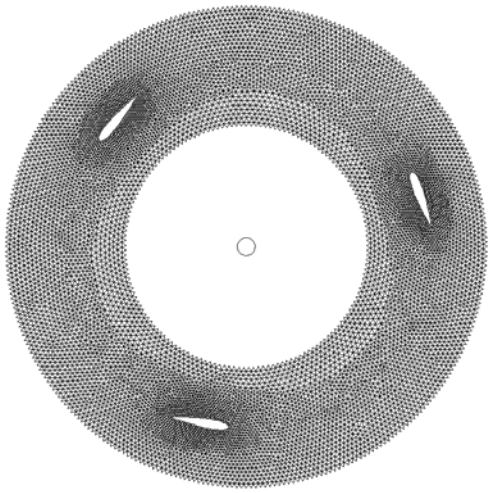

Fig. 6 Area that affected by rotor motion (New moving reference frame allocated to this area)

Table I. Rotor detail

NACA0016	Airfoil
6m	Rotor diameter
3	Number of blades
1m	Chord length
1	Solidity

IV. RESULTS AND DISCUSSIONS

Fig. 7 illustrates velocity contours in the whole domain for each case. As previous studies have shown, the rotational speed and the rotor tip speed ratio have great impact on geometry and length of rotational wakes. More rotational speed leads to less wake velocity. However, low rotational speed leads to low tip speed ratio, which make stall and generating wakes.

Fig. 8 shows velocity contours near the rotor for ω=5rad/s. As is obvious, first blade angle of attack is such that blade is under intense stall condition and flow is totally separated. Due to the separation a rotational wake generated in region (A) that showed in Fig. 8.The velocity is very low in this region and according to the Fig. 10 has a high intense of turbulence. The biggest rotational wake is related to the third blade that covered region (B) in Fig. 8. This area also has a very intense turbulence. High velocity area near the second blade is due to the direction of free stream velocity and velocity of the rotational flow that generated by rotor, in this area both of them have a same direction so they aggravate each other and make a high velocity area.

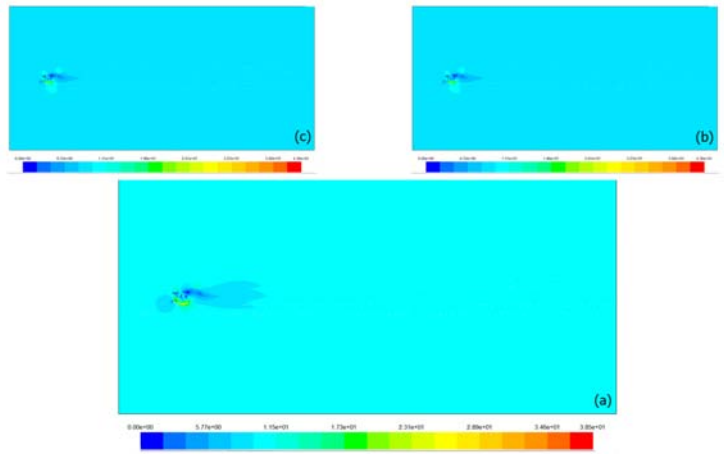

Fig. 7 Magnitude velocity contours in whole domain, (a):ω=5rad/s, (b):ω=8rad/s, (c):ω=12rad/s

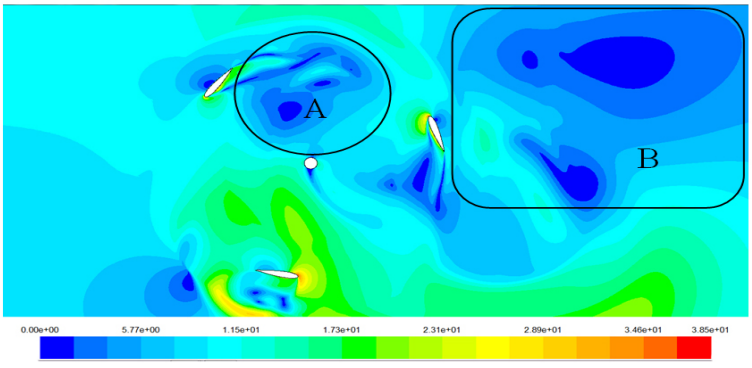

Fig. 8 Magnitude velocity contours near the rotor for ω=5rad/s

ISSN (Online): 2305-0225
Issue 15(4), August 2014, pp. 482-487

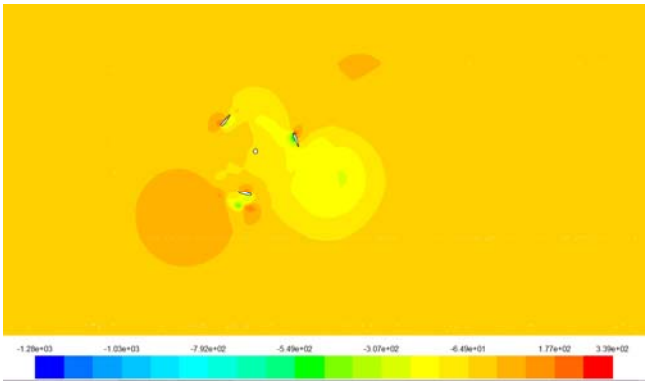

Fig. 9 Pressure contours near the rotor for ω=5rad/s

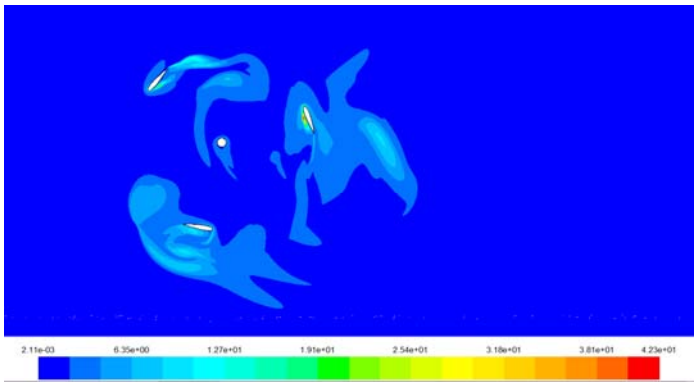

Fig. 10 Kinetic energy of turbulence contours near the rotor for ω=5rad/s

Fig. 11 is the best simulation approach that illustrates velocity triangles in Fig. 3. This image represents the path lines and shows the impact of rotor rotational speed on the free stream velocity direction and determined rotational wakes structures very well. Free up-stream with value of V_∞ and horizontal direction moves toward the rotor and become shelvy gradually in area close to the rotor. Then enter the area affected by the rotor and V_∞ transform to V that is absolute velocity of the flow in the rotor area. It is available to calculate angle of attack for first blade that showed in Fig. 11 with respecting to the linear speed of blade and velocities directions. The region (A) rotational wake in Fig. 8 path lines is obvious in Fig. 11 very clear.

Fig. 12 to Fig. 15 illustrate velocity magnitude distribution on the horizontal lines y = 0, y = 2, y = 4, y = -2, y = -4. This method could provide an adequate understanding of the size and length of the rotational wakes. Fig. 12 shows that the greatest impact of the wakes on the line passing through the axis of the rotor for rotational speed of 5 rad/s is to 25 meters far from rotor axis. After that, flow began the healing process and rotational wake completely disappears after almost 75 meters. Fig. 13 also indicates the same results that on other horizontal lines also strong affects up to 25 meters and then flow started to heal. This analysis method can be used for other rotational speeds, and the length and size of each wake could be analyzed this way.

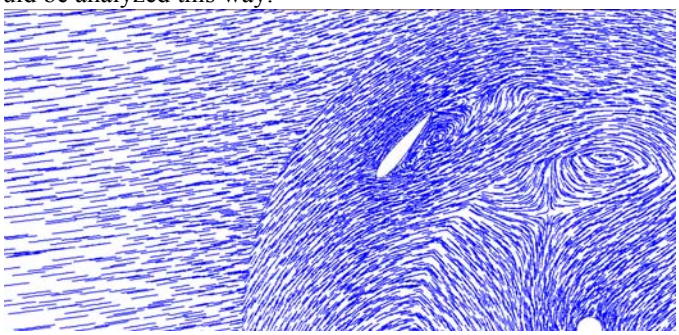

Fig. 11 Path lines near the rotor for ω=5rad/s

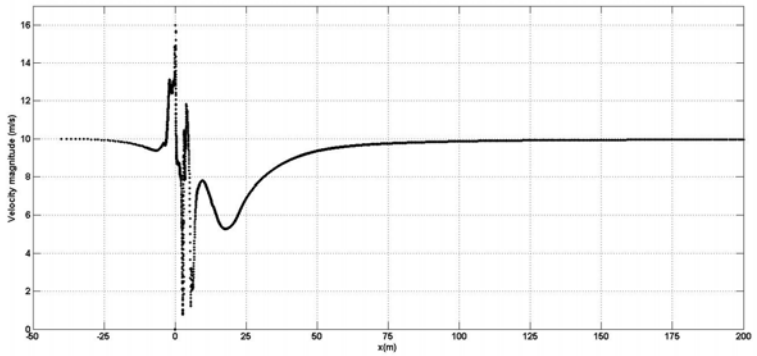

Fig. 12 Magnitude velocity distribution on y=0 line for ω=5rad/s

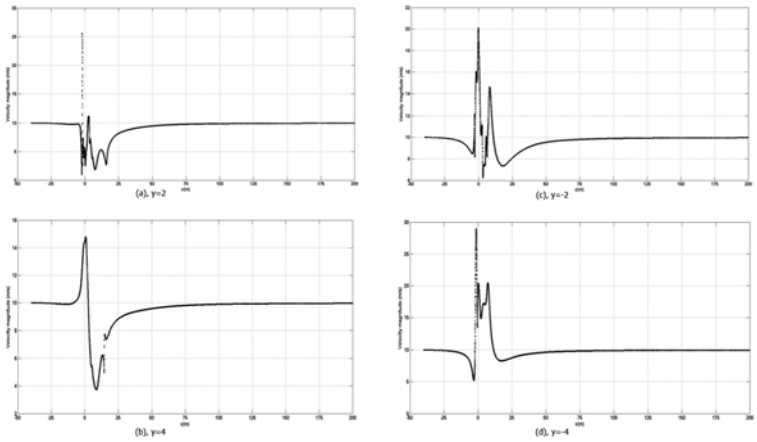

Fig. 13 Magnitude velocity distribution for ω=5rad/s, respectively on (a):y=2m, (b):y=4m, (c):y= -2m, (d):y= -4m.

ISSN (Online): 2305-0225
Issue 15(4), August 2014, pp. 482-487

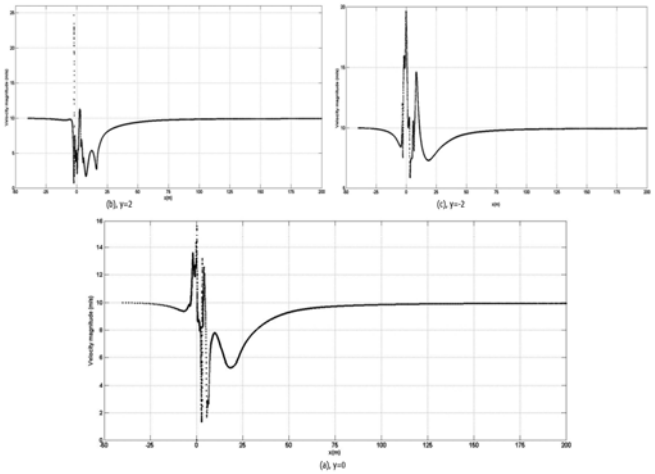

Fig. 14 Magnitude velocity distribution for ω=8rad/s, respectively on (a):y=0m, (b):y=2m, (c):y= -2m.

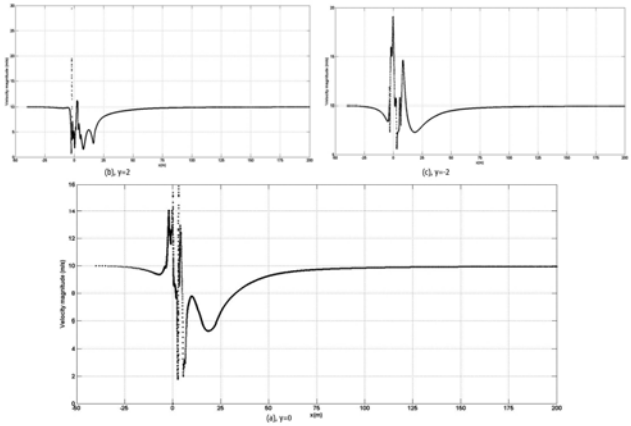

Fig. 15 Magnitude velocity distribution for ω=12rad/s, respectively on (a):y=0m, (b):y=2m, (c):y= -2m.

V. Conclusion

In this paper, a numerical computational fluid dynamics method are used to simulate flow field around a Darrieus vertical axis wind turbine with three straight blades that used NACA 00016 symmetric airfoil for estimating wake size and study impact of rotational speed of rotor on the wake lengths. Select a moving reference frame help us to prepare good results that are accommodate with real overall view. Simulation done for tree rotational speeds and velocity, pressure and turbulence contours obtained in whole domain. Also, distribution of velocity magnitude along some horizontal direction are plotted to predict wake length in each direction and provide an opportunity to study impact of rotational speed on wake size. As the path lines obtained we are able to compare numerical simulation with analytical velocity triangles. Results showed that increasing of rotational speed leads to longer and much more turbulent wakes.

References

[1] Liang Cao, Huimin wang, Yao Ji, Zhiliang Wang, Weibin Yuan(2010); Analysis on the influence of rotational speed to aerodynamic performance of vertical axis wind turbine; Procedia Engineering, (31), 245 – 250.

[2] Robert Howell, Ning Qin, Jonathan Edwards, Naveed Durrani(2010); Wind tunnel and numerical study of a small vertical axis wind turbine, Renewable Energy, (35), 412–422.–135.

[3] Marco Raciti Castelli, Alessandro Englaro, Ernesto Benini(2011); The Darrieus wind turbine: Proposal for a new performance prediction model based on COMPUTATIONAL FLUID DYNAMICS, Energy, (36),4919-4934.

[4] Muhammad Mahmood Aslam Bhutta, Nasir Hayat, Ahmed Uzair Farooq, Zain Ali, Sh. Rehan Jamil, Zahid Hussain(2012); Vertical axis wind turbine – A review of various configurations and design techniques, Renewable and Sustainable Energy Reviews,(16) ,1926–1939.

[5] Chao Li, Songye Zhu, You-lin Xu, Yiqing Xiao(2013); 2.5D large eddy simulation of vertical axis wind turbine in consideration of high angle of attack flow, Renewable Energy, (51), 317-330.

[6] Babadi Soultanzadeh, Milad; Mehmandoust Isfahani, Babak; Selecting optimum wind turbines airfoil for using in low speed winds, first conference of new and clean energies(2013). its available on http://www.civilica.com/Paper-CCE01-CCE01_074.html.

[7] Crespo, Hernandez(1996); Turbulence characteristics in wind turbine wakes, Journal of Wind Engineering and Industrial Aerodynamics, (61), 71-85.

[8] Magnusson, Smedman(1999); Air flow behind wind turbines, Journal of Wind Engineering and Industrial Aerodynamics, (80), 169-189.

ISSN (Online): 2305-0225
Issue 15(4), August 2014, pp. 488-492

The effect of the compositions of sowing bed on germination, vitality, and viability factors of *Pinus nigra* Arnold with provenances of Urmia and Kelardasht in Nursery of Mahabad's Darlak

Foroogh Bahmani, Abbas Banj Shafiei, Javad Eshaghi., and Majid Pato

***Abstract*—** The present study has been done with aim to investigate the effect of different treatments of sowing bed on seeds and seedlings of *Pinus nigra* Arnold with provenances of Urmia and Kelardasht in Darlak nursery of Mahabad. To reach this purpose, the seeds were planted in plastic pots in 5 replications of completely random pattern with 4 different treatments including: control treatment "soil 1: muck 1: sand 1", treatment 1 "soil 1: muck 1: sand 2", treatment 2 "soil 1: muck 1: sand 4", and treatment 3 "pure sand". The results showed that the best seed germination traits of *Pinus nigra* Arnold was in sand sowing bed (treatment 3). Also the highest percentage of viability and seedlings with good degree of quality was in sandy sowing bed (treatment 3). From such results this can be concluded that the sandy sowing bed improves physical conditions of soil and increases germination rate, vitality, and viability of *Pinus nigra* Arnold with provenances of Urmia and Kelardasht.

***Keywords*—** sowing bed; germination; vitality; viability; *Pinus nigra* Aronold.

I. INTRODUCTION

"Plantation" is very important around the world, so that the plantation areas comprise about 10% of the world's forests [11]. In a country such an Iran, the development of the conifers and deciduous species forests is considered as one of the main objectives. The main goals of plantation of conifer species in Iran are issues as: soil's conservation and fertility, constructing green spaces and promenades in the suburbs, clearing the air, production of wood, restoration of degraded forests, improvement of quality and enrichment of forestry stand for mass production of industrial wood, increase of yield per surface unit, creating forestry parks and conserved forests and restoration of degraded forests of totally vanished forests [4, 6, and 7]. *Pinus nigra* Arnold is one of the valuable coniferous species of dry and semi dry lands that could grow up to 2000 meter of sea level and its natural habitat is mostly central and southern foothills of Europe. Due to its great ecological flexibility, it shows good resistance not in cold and glacial weather, but often grows well in calcareous soils and has strong and proper roots, and the other hand, some species, varieties, and its other provenances could grow in acid soils. *Pinus nigra* Arnold's ecological needs to soil moisture and nutrients are very low [5]. According to the use of human plantation after reach to a new and somehow stable ecosystem, it should be of great importance to pick up proper and adaptable spices with great viability and preferred growth [4]. The success of all these programs depends to production of seedlings with appropriate quantity and quality characteristics in the nursery. There are several factors that are effective in quantity and quality of produced seedlings such as, "sowing bed" which is done through optimization of soil physical condition that could improve germination of seed, growth of root, and production of seedlings [17 and 18]. Studies show that soil amendment is one of the most important ways for the success of plantation management. Rooting, growth and primary establishment of improved seedlings and their resistance against moisture, heat, and disease tension is increased through this practice [14]. Therefore, the present study intends to introduce best composition for better establishment and growth of *Pinus nigra* Arnold's seedlings with provenances of Urmia and Kelardasht through examination of different soil treatments.

II. MATERIALS AND METHODS

This research has been done in Darlak nursery located 20 km from Mahabad city (43 ° 45 East and 55 ° 36 North), with an altitude of 1288 meters above sea level and average annual rainfall of 410/2 mm and average annual temperature of 13/3 ° C. In this experiment, the *Pinus nigra* Arnold seed provenance of Kelardasht with 89% viability, and seed weight of 12 g and seed provenance Urmia with 76% viability and seed weight 2/19 grams purchased from Caspian Forest Seed Centre then,

ISSN (Online): 2305-0225
Issue 15(4), August 2014, pp. 488-492

4 different compositions of sowing bed according to Table 1 has been prepared. Then three seeds were planted in each pot (40 pots in total) with 10*15*25 cc dimensions in a completely random pattern with 5 replications, under sawdust seed cover, February planting date, and irrigation per day conditions. Before planting seeds and pots' soil (sowing bed) were disinfected with Benom.yl, a sample has taken from each treatment after pot's soil preparation and has been sent to soli laboratory to determine physical and chemical feature (Table 2). Seed counting has started late April (after observation of the first germinated seed) and has repeated every week until the germination of the all seed with viability power. Needed care has taken such as everyday irrigation with the beginning of dry season from April and weeding operation (manually). After germination of seeds (late June), attempts has made to maintain a seedling in each pot (by removing other seedlings). Measurement of the process of viability at the end of the growing season in terms of percentage has been calculated by means of counting the number of seedlings in each replication of soil and assigning Grade 1 for survived seedlings and Grade 2 to not-survived seedlings [16]. With use of Table 3, quality of seedlings (vitality) has been recorded. In order to assess the most important indicators of potential germination factors, germination percentage factors, everyday mean germination, the maximum daily germination, speed of germination [19], the energy of germination [13], the value of germination [12] were determined according to the researchers listed in Table 4.

A. Statistical Analysis

After measuring the parameters, the data were recorded using Spss 18 software and with Box plot command outliers were identified and removed. KS test was used for the detection of data normality, in the case of normal data, one-way ANOVA analyze were used to evaluate the significance of differences between treatments, if there were significant differences among treatments, Duncan mean comparison test was applied. In addition, agreement Tables (Crosstabs) was used to analyze the data of vitality.

III. RESULT

A. Germination factors

results of the ANOVA test of the effect of sowing bed at the 5% level (control, treatment 1, treatment 2 and treatment 3) on germination factors showed that at different levels of sowing bed treatments on all germination parameters including germination percentage, mean daily germination, speed of germination, the maximum mean of daily germination, the germination percentage and germination energy, in both the seed sources under investigation has a meaningful influence during the test period (see Table 5).

Also, Mean germination comparison results in Duncan levels showed that mean germination factors in treatment 3 was the most observed treatments among others and had significant difference with 95% confidence level (see Table 6).

B. Viability and vitality of seedlings

The results showed that only seeds with provenances of Urmia, treatment 3 (sand sowing bed) had 80% germination and 60% viability until the final levels of test period but other reminder treatments had not. Also study on frequency distribution of two sowing bed and vitality at the end of growing season showed that from 3 seedlings in treatment 3, 1 (33.3 %) ranked in good category and 2 (66.7 %) in medium category (see Table 7).

Also study on seeds with provenances of Kelardasht showed that treatment 3 (sand sowing bed) had 80 % germination and 80 % viability until the final levels of the test period but no other treatments had such an influence. Also the frequency distribution of two factors of sowing bed and vitality at the end of growing season showed that from 4 seedlings in treatment 3, 2 (50%) ranked in good category, 1 (25%) in medium category and 1 (25%) in bad category (see Table 8).

IV. DISCUSSION

Sowing bed cinder as one of the influential elements in growth and viability of seedlings and it could increase the chance of the plantation success [10]. In this study, the type of pot's soil (sowing bed) had a meaningful effect on seed germination characteristics of Pinus nigra Arnold however the calculated amount of germination characteristics in control treatment, treatment 1, and treatment 2 had prominent differences as compared with treatment 3. So the sowing bed which is formed by sand (treatment 3) is a preferred bed for germination of this species seed and it could improve its total germination characteristics. As pines are among the trees which have a low need to heat, moisture, and water and appropriate soil conditions and their original habitat is loam soils and poor environments of nutritious elements [7] perhaps other treatments due to higher clay content (Table 2) provide the ability to absorb more water, and due to higher moisture they did not provide favorable conditions for germination of Pinus nigra Arnold. On the other hand, sand bed due to being lighter and providing better rooting and also its proper drainage could provide a suitable environment for seed germination and put the plant in more better conditions. Sand bed is very poor at retaining water [3], and this advantage is likely to provide favorable conditions for seed germination of Pinus nigra Arnold. Furthermore, higher levels of vitality and viability in treatment 3 (sand bed), suggesting that the Pinus nigra Arnold bed prefers a sowing bed with good drainage and it evades high humidity. These may be different in other

ISSN (Online): 2305-0225
Issue 15(4), August 2014, pp. 488-492

species, so that organic materials could increase speed of germination and resistance of seedlings through improvement of nutrition and physical feature of soil and consequently increase plant production efficiency (quantitative and qualitative) of Pinus brutia, Pinus halepensis, Cupressus sempervirens [1, 2, 15, 20]. Also Tabari et. al [9] in a study on the effect of 4 different soils on the amount of production of Cupressus sempervirens seedling and height growth of this species in the Shahrposht nursery of Noshahr concluded that clay-loamy-sandy in comparison with sandy soil has higher viability, height growth and nutritious elements because of its lighter weight and more rooting improvement.

APPENDIX

Table 1 - Ratio of soil components in different compositions of soil experimental treatments

Treatment name	Soil	Muck	Sand
Control	1	1	1
Treatment 1	1	1	2
Treatment 2	1	1	4
Treatment 3	-	-	1

Table 2 – Treatment's characteristics of soil pots (seed bed)

Treatments	Control	Treatment 1	Treatment 2	Treatment 3
Soil texture	SL	SL	LS	LS
Sand %	61.7	71.7	74.2	79.2
Silt %	20	15	12.5	12.5
Clay %	18.3	15.8	13.3	5.8
Potassium Mg/kg	1281	1026	823	47
Phosphorus Mg/kg	28.8	23.6	19	1.6
Nitrogen %	0.18	0.12	0.1	0.01
Organic materials %	3.1	2	1.8	0.17
Calcium carbon %	8.4	8.7	8.8	9.1
EC dS/m	1.72	1.24	1.23	1.03
PH	7.4	7.48	7.52	7.55

Table 3 - Criteria for the classification of seedlings vitality (Soofizadeh et al., 2009)

PERCENTAGE OF TOTALLY COMPLETE GREEN SCALES (PERCENT)	VITALITY
68-100	GOOD
33-67	AVERAGE
0-32	BAD

Table 4- Computational relations of characteristics under investigation

Characteristics under investigation	Method of characteristics calculation
Germination rate	$\text{Germination rate} = \frac{n_i}{N} \times 100$
Mean daily germination	$\text{Mean daily germination (MDG)} = \sum \frac{Cpsgt}{T}$
Maximum mean daily germination	$\text{Maximum mean daily germination (PV)} = \frac{Cgp}{n_i}$
Germination speed	$\text{Germination speed} = \sum \left(\frac{n_i}{n_i}\right)$
Germination energy	$\text{Germination energy} = \frac{n_i}{N} \times 100$
Germination value	$\text{Germination value} = \text{final MDG} \times PV$

Germinated seeds during the period, (Ni) equals the number of germinated seeds in a given time ti, (N) equals the number planted seeds, (ti) equals the number of days after the beginning of germination process, (Cpsgt) equals the percentage of the germinated seeds over the period, (Pv) equals the maximum mean of germination over the germination process, (T) equals total period of germination and (Cgp) equals the cumulative percentage of germination in the counting day.

Table 5- ANOVA test of effects of different treatments of sowing bed on germination factors of *Pinus nigra* Arnold with provenances of Urmia and Kelardasht

	Urmia provenance		Kelardasht provenance	
Germination indices	F	Sig	F	Sig

ISSN (Online): 2305-0225
Issue 15(4), August 2014, pp. 488-492

Germination rate	6.722	0.004*	6.305	0.005*
Mean daily germination	7.122	0.003*	3.608	0.037*
Germination speed	13.467	0.000*	8.885	0.001*
Maximum mean daily germination	10.411	0.000*	6.394	0.005*
Germination value	5.968	0.006*	3.396	0.044*
Germination energy	6.722	0.004*	6.305	0.005*

* indicates meaningfulness of means when α= 0.05

Table 6- Indicators of germination means in Urmia and Kelardasht provenances

		Germination rate	Mean daily germination	Speed germination	Maximum mean daily germination	Germination value	Germination energy
Urmia	Control	46.66^{ab}	2.91^{ab}	0.08^{b}	2.91^{b}	16.48^{b}	46.66^{ab}
	Treatment 1	6.66^{b}	0.44^{bc}	0.01^{b}	0.44^{b}	0.98^{b}	13.33^{b}
	Treatment 2	6.66^{b}	0.22^{c}	0.00^{b}	0.22^{b}	0.24^{b}	6.66^{b}
	Treatment 3	86.66^{a}	5.02^{a}	0.28^{a}	7.64^{a}	40.65^{a}	86.66^{a}
kelardasht	Control	19.99^{b}	3.08^{ab}	0.09^{b}	3.08^{b}	18.60^{ab}	19.99^{b}
	Treatment 1	6.66^{b}	0.22^{b}	0.00^{b}	0.22^{b}	0.24^{b}	6.66^{b}
	Treatment 2	39.99^{ab}	1.67^{ab}	0.05^{b}	1.67^{b}	5.83^{b}	39.99^{ab}
	Treatment 3	73.32^{a}	4.82^{a}	0.20^{a}	6.01^{a}	30.86^{a}	73.32^{a}

Different letters indicate meaningfulness of means with 95% confidence level
Treatments' composition (soil:muck:sand)= Control (1:1:1), treatment 1 (1:1:2), treatment 2 (1:1:4), treatment 3 (sand)

Table 7- Crosstabs of sowing bed * vitality of Urmia provenance

			Quality (02/08/91)			total
			Good	Medium	bad	
Seed bed	Treatment 3	Count	1	2	-	3
		% within seed bed	33.3%	66.7%	-	100 %
		% within quality (02/08/91)	100%	100%	-	100 %
		% of total	33.3%	66.7%	-	100 %
total		Count	1	2	-	3
		% within seed bed	33.3%	66.7%	-	100 %
		% within quality (02/08/91)	100%	100%	-	100 %
		% of total	33.3%	66.7%	-	100 %

Table 8- Crosstabs of sowing bed * vitality of Kelardasht provenance

			Quality (02/08/91)			total
			Good	Medium	bad	
Seed bed	Treatment 3	Count	2	1	1	4
		% within seed bed	50%	25%	25%	100%
		% within quality (02/08/91)	100%	100%	100%	100%
		% of total	50%	25%	25%	100%
total		Count	2	1	1	4
		% within seed bed	50%	25%	25%	100%
		% within quality (02/08/91)	100%	100%	100%	100%
		% of total	50%	25%	25%	100%

REFERENCES

[1] Ahmadloo, F., Tabari, M., Rahmani, A., Yousefzade, H., Razagh zadeh, M., 2009b. Effect of soil composition on seed germination of *Pinus halepensis* Mill. Iranian Journal of Forest and Poplar Research, Vol. 17(3): 394-403 (in persian).

[2] Ahmadloo, F., Tabari, M., Rahmani, A., Yousefzade, H., 2009c. Study of seed germination and seedling survival of *Pinus brutia* Ten. In different soils of nursery. J of Wood & Forest Science and Technology, Vol. 16(3): 61-76 (in Persian).

[3] Ardakani, M.R., Ecology. University of Tehran Press 14th Ed, 340 p.

[4] Czabator, F.J., 1962. Germination value: an index combining speed and completeness of pine seed germination. Forest Sci., 8: 386-396.

[5] Dastmalchi, M., Sagheb talebi, Kh., Vaziri, A., Vab, D., Latifi, M., Diyanat nezhad, A., Sardabi, H., 1997. Survey on adaptability of native trees in Guilan province: The results of adaptablity tests of trees' specious (Coniferus). Research institue of forests and rangeland, No 169: 76-136.

[6] F.A.O., 1985. A guide forest seed handling. http://www.fao.org/docrep/006/AD232E/AD232E10.htm.

[7] Floistad, I.S. and Kohmann, K., 2004. Influence of nutrient supply on spring frost hardiness and time of bud break in Norway spruce (*Picea abies* (L.) Karst.) seedlings. New Forests, 27: 1-11.

[8] Hassan, H.A., Mohamad. S.M., Abo. El. Ghait. Em.,Hammad. H.H., 1994. Growth and chemical composition of *Cupressus sempervirens* L. seedlings in response to growing media, Annals of Agricultural Science, Moshtohor, Egypt, 32: 497-509.

[9] Khademi, A., Adeli, E., Babaei, S., Mattaji, A., 2006. Study of afforestation (Khojin Forest park & Hiroabad) in Khalkhal area and present adaptable species. Journal of Agricultural Sciences, 11 No 4.

[10] Larcheveque, M., Ballini, C., Korboulewsky, N., and Montes, N., 2006. The use of compost in afforestation of Mediterranean areas: Effects on soil properties and young tree seedlings. Science of the Total Environment, 369: 220-230.

[11] Mollashhi, M., Hosseini, S.M., Naderi, A., 2009. Effect of seed provenances on germination, height and diameter growth of wild cherry *(prunus avium* L.) seedlings. Iranian Journal of Forest and Poplar Resesarch Vol. 17 No. 1.

[12] Mosadegh, A., 1999. Plantation and forest nurseries. Tehran University Press, 516 p.

[13] Nambiar, E.K.S. and Fife D.N., 2007. Growth and nutrient retrains location in needles of radiate pine in relation to nitrogen supply. Soil Science Society of America Journal, 60: 147-156.

ISSN (Online): 2305-0225
Issue 15(4), August 2014, pp. 488-492

[14] Oliet, A.J., Planelles, R., Artero F. and Jacobs F.D., 2005. Nursery fertilization and tree shelters affect Sclerotiniasclerotiorum. Plant Pathology, 48: 77-82.
[15] Panwar, P. and Bhardwaj, S.D., 2005. Handbook of practical forestry, Agrobios, India, 191 p.
[16] Rezaei, A., 2001. Growth and yield study of *Picea abies* in Lajim district. Iranian Jornal of Pajouhesh & Sazandegi No: 48, pp: 56-59.
[17] Sardabi, H., 1998. Study of adaptability of different Eucalyptus Species and Pine in Coastal and low height regions of eastern Mazindaran. Research institue of forests and rangeland, No: 198, 133 p.
[18] Soofizadeh, N., Hoseini, S.M., Tabari, M., 2009. Effect of sowing date, irrigation and weed control on biomass, ratio of shoot/root length and vitality rate of seedling *Cupressus arizonica* in nursery. Iranian Journal of Forest, Vol. 1, No. 2, 163-173.
[19] Tabari, M., Poormajidian, M. R., Alizadeh, A. R., 2004b. Effect of soil, irrigation and weeding on production of cypress (*Cupressus sempervirens* L.) seedling in shahrposht Nursery, Nowshahr. Pajouhesh & Sazandegi No: 70, pp: 56-69 (in Persian).
[20] Tabari, M., Saeidi, H.R., Basiri, R. 2004. Response of cypress (*Cupressus sempervirens* var. horizontalis) seedlings to soil type and planting depth in plain areas of Caspian sea. Proceedings of the Fourth International Iran & Russia Conference, 1061-1066.

Foroogh Bahmani MSc in Forestry from Urmia university, BSc in Forestry from Shahid Chamran university.

ISSN (Online): 2305-0225
Issue 15(4), August 2014, pp. 493-498

Improved hybrid electric system using soft switching

A. Beiki, M. Niroomand

***Abstract*—**In this paper, an improved hybrid system is presented. main Energy source is a fuel cell but Due to fuel cell constraints and slow dynamic, Use it alone is not appropriate. To solve this problem, battery and super capacitors are used as auxiliary sources inside fuel cell.The strategy is based on dc link voltage control. Therefore, there are three voltage control loops: dc bus voltage regulated by a super capacitor bank, super capacitor voltage regulated by a battery bank, and battery voltage regulated by a FC. Each source is connected to dc bus by dc to dc converter. Converters are key part of system management. Since fuel cell is the main part of hybrid system so its converter is very important.in this paper we introduce a soft switching boost converter for fuel cell. This converter reduces system losses and lower fuel consumption. The results were simulated using MATLAB SIMULINK. Simulation of whole management system structure with soft switching scheme show reduction in losses and improvement system performance.

Keywords— hybrid electric system, energy management, dc-dc converters, soft switching.

I. INTRODUCTION

In recent years due to concerns about restrictions on the use of fossil energy sources, renewable energy has risen sharply. Among the renewable energy sources, Fuel cell has high popularity in Transportation applications. using batteries and super capacitors along with fuel cell have higher efficiency combustion engine hybrid system combined with an electric generator. Most popular fuel cell for use in transportation is (PEMFC). Batteries and super capacitors, are most conventional auxiliary energy sources, along with the fuel cell in electric vehicles. In order to provide an initial transient peak power or capture energy from the bus, a super capacitor, is required. Super capacitors are with high energy density but low power density than batteries. So use these resources together to offer the best combination of power hybrid system.

Application of FCs in vehicle is one of the promising solutions to provide a high energy efficient, quiet, less pollutant and electric vehicle with longer driving range (as long as the fuel supply is available). The Polymer electrolyte membrane Fuel Cell (PEMFC) is commonly utilized in the FCEV due to its relatively small size, light weight and simple structure . PEMFC generates electricity through the chemical reaction between hydrogen and oxygen. Hence, the by-products from it contains of heat and water. However, there are problems when one tries to use FC alone to power the vehicle, such as its relatively short lifespan, poor dynamic response, and difficulty during FC cold startup, high cost, and inability to capture of braking energy during vehicle deceleration or down hill . Moreover, peak power demand from the FC could lead to fuel starvation phenomenon and shorten its lifespan. For these reasons, hybridization of FC with energy storage units (ESUs) is necessary in order to overcome these problems as well to reduce the vehicle size and cost.

In systems which a dc-dc converter is placed between the power sources and the bus, power rotating control between resources and between resources and the bus is much better to do. in various articles different models of hybrid systems such as fuel / battery fuel cell/capacitor and fuel cell / battery / super capacitor has been discussed , but in none of the articles their dc-dc converters has been discussed in detail . in this paper we introduce a dc-dc converter with soft switching for fuel cell as main source of steady state energy. introduced converter reduces converter switching losses and improves working conditions of sources.

II. STRUCTURE OF HYBRID SYSTEM

Desired structure is formed of various power sources and control .Each section will gradually be discussed at length. We will first introduce the sources and converters. As shown in Figure 1, the system is formed three sources : battery / fuel cell / super capacitor . Any resources are connected to the bus by dc-dc converters.

III. . CONTROL STRUCTURE

Control structure and sources of power, are shown in Figure 2. Fuel cells as main energy source are connected to the dc bus by soft switching converters. Given the dynamics of the fuel cell for powering the bus is slow resources (batteries and super capacitors) are intended for parallel connection to the bus. Batteries and super capacitors are connected to the bus using bi-directional converters. This type of connection allows

ISSN (Online): 2305-0225
Issue 15(4), August 2014, pp. 493-498

us to control the charge and discharge process. The main task of rotation and energy transfer between the sources and the bus is the responsibility of dc-dc converters. Control of output voltages and currents of sources is done by switching the dc-dc converters. Final output loop pwm controller for Tuesday

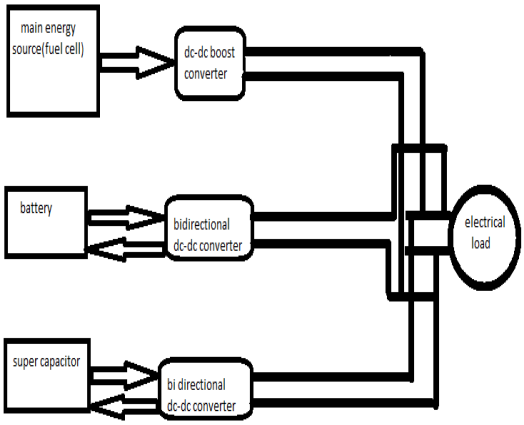

Fig.1 structure of hybrid system

converters provide three references. final output of control loops provide Three current reference for loop converters pwm loop. As well the overall structure has three reference voltage: Bus reference voltage, battery reference voltage and super capacitor reference voltage battery that supplies are rated according to capacity. Continue to introduce the system control components described below. In the following we will introduce the system control components.

A. battery voltage control loop

As shown in figure 3 the goal of this loop is to provide a current reference for the battery charging loop. During this loop, at first the battery voltage is measured and after passing through the filter is compared with battery reference voltage. High-pass filter is placed to eliminate the battery current distortion which is due to the bidirectional converters switching. In the absence of measured filter voltage enters controller with high error. P controller is used to boost the voltage error. Controller generates the desired current reference. In The proposed system the fuel cell adjusts battery state of charge.

B. battery charging control loop

Reference current resulting from the previous control loop will enter to the battery charging loop and is compared with battery current Figure 4. Measured battery current must pass through the filter to avoid entering distortion in the controller.in The loop input measured battery current is multiplied by -1 to charge and discharge of the battery for the control system to be understood. Finally, according to the characteristics of the fuel cell current limit is determined. by the limiter. Due to the dynamics of the fuel cell a limiting current slope is placed before pwm loop to avoid fuel cell from damage.

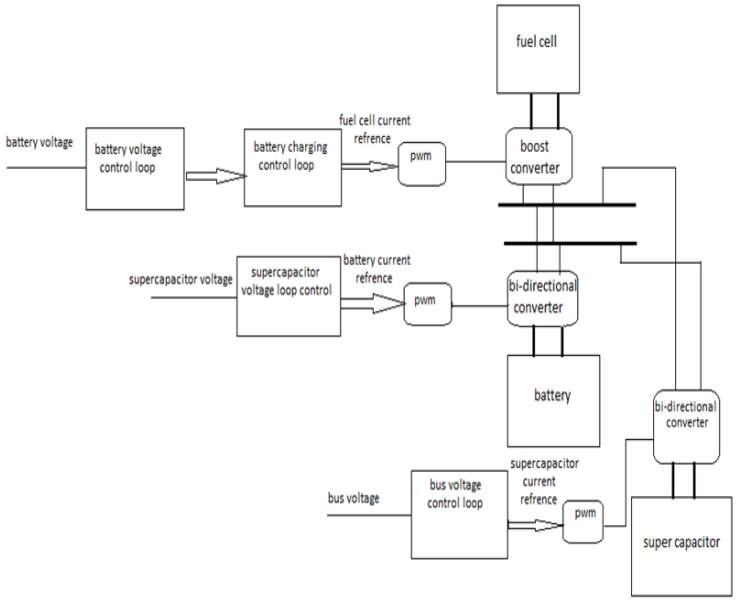

Fig.2 power and control structure of system

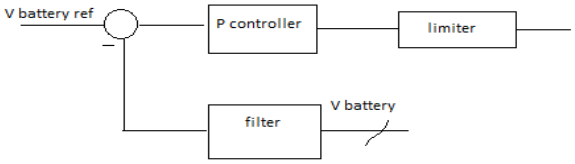

Fig.3 battery voltage control loop

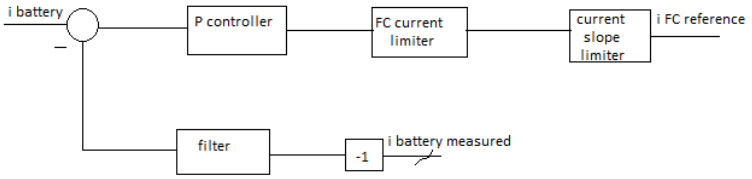

Fig.4 battery charging control loop

C. Super capacitor voltage control loop

The main goal of this loop is to regulate the status of battery charge and discharge. Note that setting the charge level of the super capacitor is for lithium-ion battery, super capacitor voltage reference is entered to the loop. Super capacitor voltage after passing through the high-pass filter is compared with a reference voltage and the resultant error is introduced into a pi controller. like fuel cell maximum charge and discharge current of the battery is determined according by the nominal values and capacity of the battery.by this way possible damage to the battery during charging and discharging is much safer. Steep increase in the charge and discharge currents are controlled by limiting the slope of

ISSN (Online): 2305-0225
Issue 15(4), August 2014, pp. 493-498

current. Finally, the battery reference is entered pwm loop.figure5.

D. bus voltage control loop

Reference energy with the help of reference voltage is calculated from the following equation:

$$E = \frac{1}{2} C_{bus\,ref} V^2_{bus\,ref} \quad (1)$$

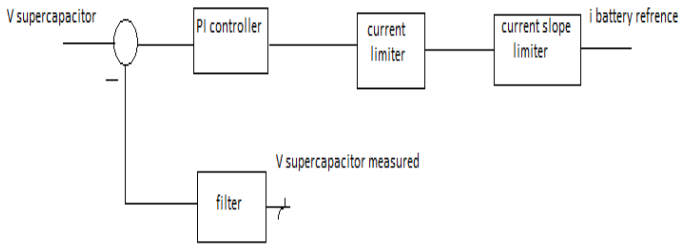

Fig.5 super capacitor voltage control loop

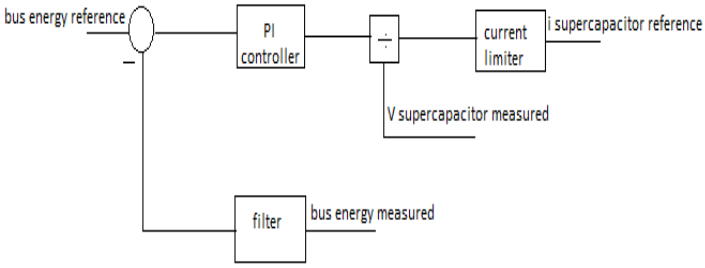

Fig.6 bus voltage control loop

IV. POWER STRUCTURE

A. *fuel cell and its converter*

Fuel cell is an electrochemical device that the reaction between hydrogen and oxygen produce dc voltage. Then we use fuel cell as a dc voltage .One of the disadvantages of fuel cell is slow start up. According to these characteristics of the fuel cell are not allowed to be used alone in the vehicles. until the chemical reaction in the fuel cell continues voltage establish .as fuel cell is the main energy source for connection fuel cell to the dc bus we use a soft switching boost converter to increase system efficiency. The proposed converter and conventional boost converter are shown in Figure 7. in all power structures proposed in various articles the conventional boost converter is used for the fuel cell. Considering that the fuel cell is main energy source using soft switching converter increases system efficiency as well. One of the advantages of the proposed converter is reduced input current ripple due to the existence of two inductor.One resonant inductor, two capacitors, and two diodes are added to a conventional boost converter for soft switching using resonance.

B . *Battery and its converter*

Battery has a high energy density and low power density. Bidirectional converter is used to connect the battery to the bus. This converter is capable to flow current to the bus and charge the battery at certain level. Kind of the battery used in this article is lithium ion the model is available in the Matlab software. during the initial moments which the fuel cell energy is not yet available battery provides energy to the bus. (1)

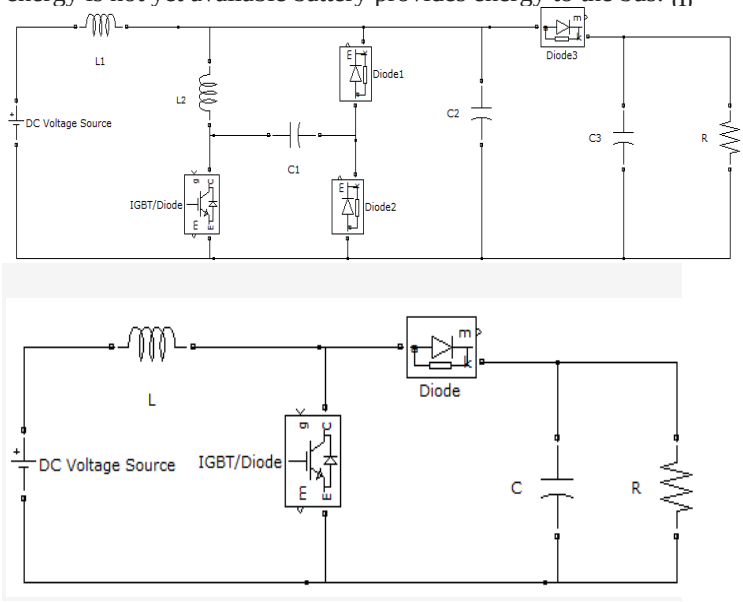

Fig.7 soft and conventional boost converter

C. *super capacitor and its converter*

Battery has a high energy density and low power density. Bidirectional converter is used to connect the battery to the bus. This converter is capable to flow current to the bus and charge the battery at certain level. Kind of the battery used in this article is lithium ion the model is available in the Matlab software. during the initial moments which the fuel cell energy is not yet available battery provides energy to the bus. A bidirectional converter is shown in figure8.

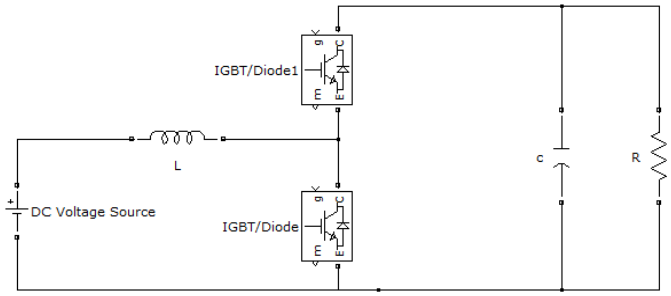

Fig.8 bidirectional converter

V. SIMULATION

Simulations in this paper is divided into two parts: First, we have evaluated the proposed boost converter features and comparison with conventional Boost, and the second part, the entire system along with all the supplies and converters are

ISSN (Online): 2305-0225
Issue 15(4), August 2014, pp. 493-498

simulated. Below two converters with their control circuits are shown. For both circuit sources, fuel cell is used as a voltage source to be more realistic simulation results. In order to control the output voltage of the converters same control method is used for both. The inductor current and output voltage feedback is taken. Voltage and current measurement are entered into the control loops. In each loop a pi controller is used and control process is completed using pwm. converters parameters are shown in table1and2. In each circuit a 6kw,45vdc PEM fuel cell is shuch as source voltage.circuits and control structures are shown in figure9.

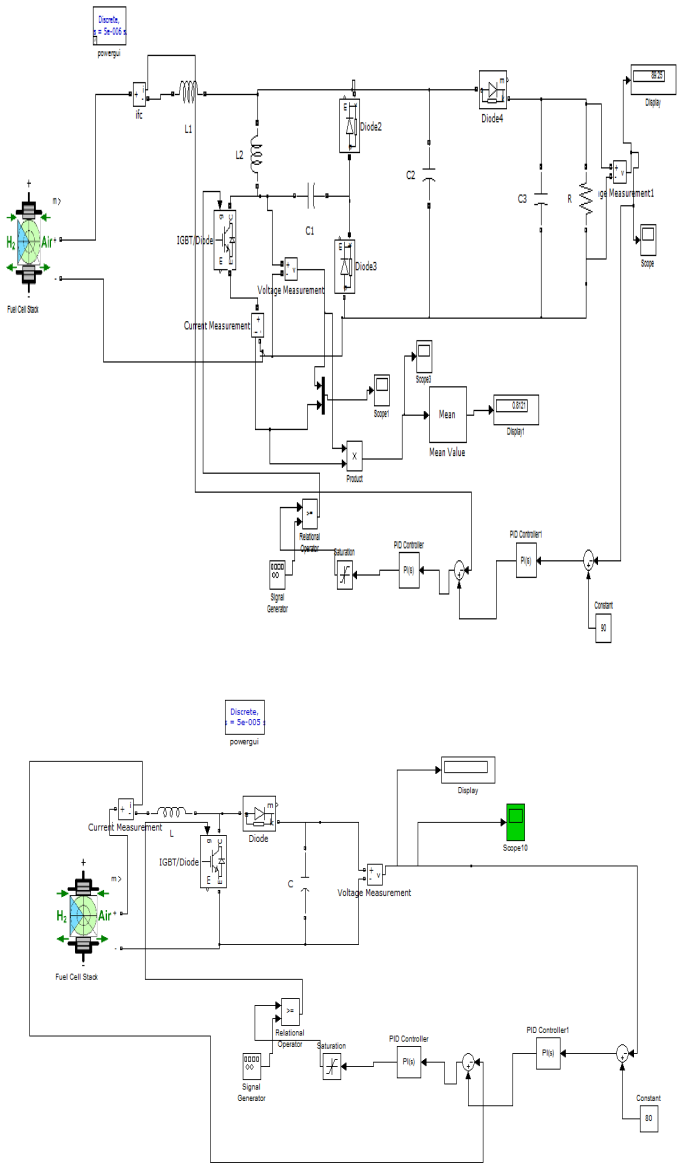

Fig.9 soft and conventional boost converter with thire control circuit

Table1,2 boost converter parameters

L1	1mH
L2	500µH
C1	100nF
C2	10nF
C3	100µF
R	10?

L	100µH
C	100µF
R	10?

The out put voltage and switch power loss of each converter is shown in figure 10and11. As can be seen in the proposed converter, the voltage transient response is improved and lower switching losses.

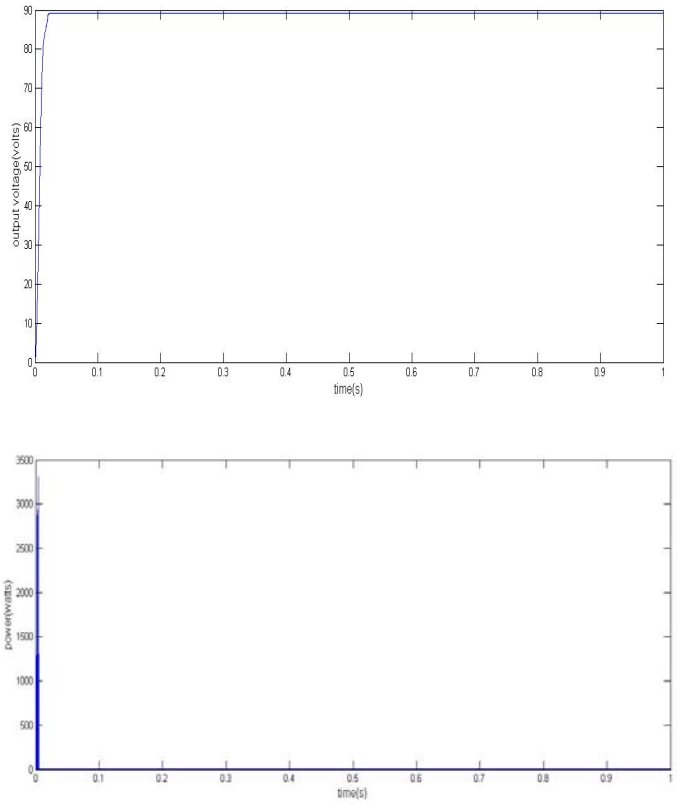

Fig.10 output voltage and switch power loss of soft boost converter

ISSN (Online): 2305-0225
Issue 15(4), August 2014, pp. 493-498

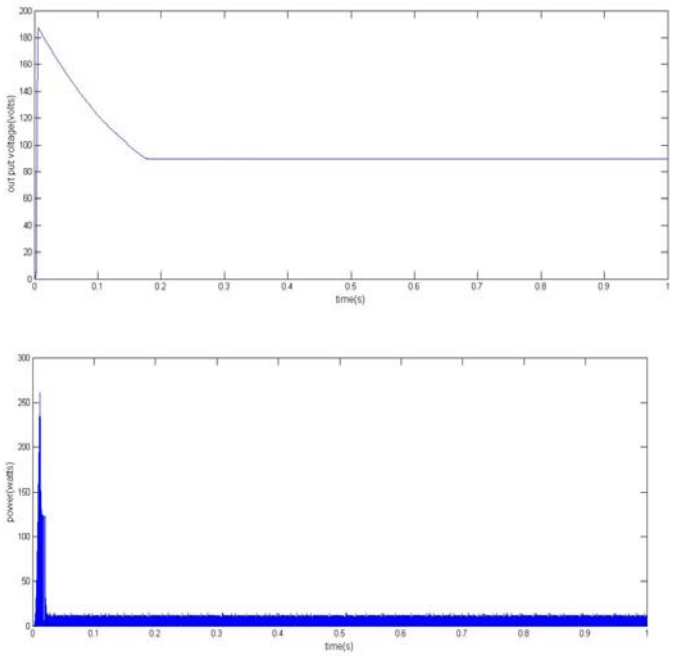

Fig.11 output voltage and switch power loss of conventional boost converter

The simulation of the entire system which is shown in Figure 2, Is done with a combination of power and control circuits. Targeting control system to maintain system voltage at the desired value. Parameters are summarized in Table 3. A 5 ohm resistor as the load on the output is considered. During the figure 12 bus voltage and current of the fuel cell when using conventional boost converter is shown., And the same values in Figure 13 when the proposed boost converter is used.it is clear that the status of bus voltage and transient fuel cell current is improved by the proposed converter.

Table3**,**whole system parameters

$V_{bus\ ref}$	42V	$I_{fuel\ cell\ min}$	0A
$V_{battery\ ref}$	30V	$I_{fuel\ cell\ max}$	20A
$V_{super\ C\ ref}$	25V	$I_{battery\ min}$	-18A
$I_{battery\ charg}$	-6A	$I_{battery\ max}$	10A
$I_{battery\ discharge}$	20A	$V_{super\ C\ min}$	20V
$I_{super\ C\ rated}$	180 A	$V_{super\ C\ max}$	35V

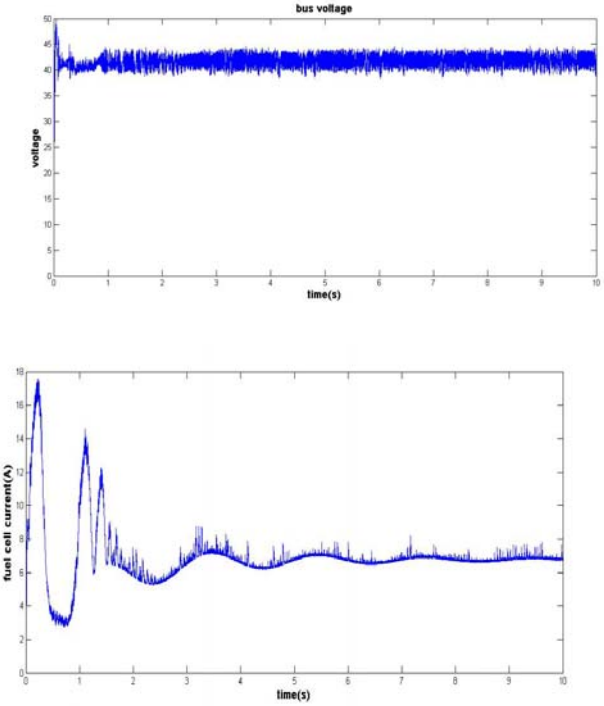

Fig.12 bus voltage and fuel cell current when conventional boost is used

VI. CONCLUSION

The key objective of this present work is to propose a soft switching boost converter for fuel cell.as fuel cell is the main energy source of hybrid system so its converter is very important. The amount of energy extracted from the fuel cell passes through the converter so soft switching of this converter reduce losses of the system effectively as well as improving transient state of fuel cell current.

ISSN (Online): 2305-0225
Issue 15(4), August 2014, pp. 493-498

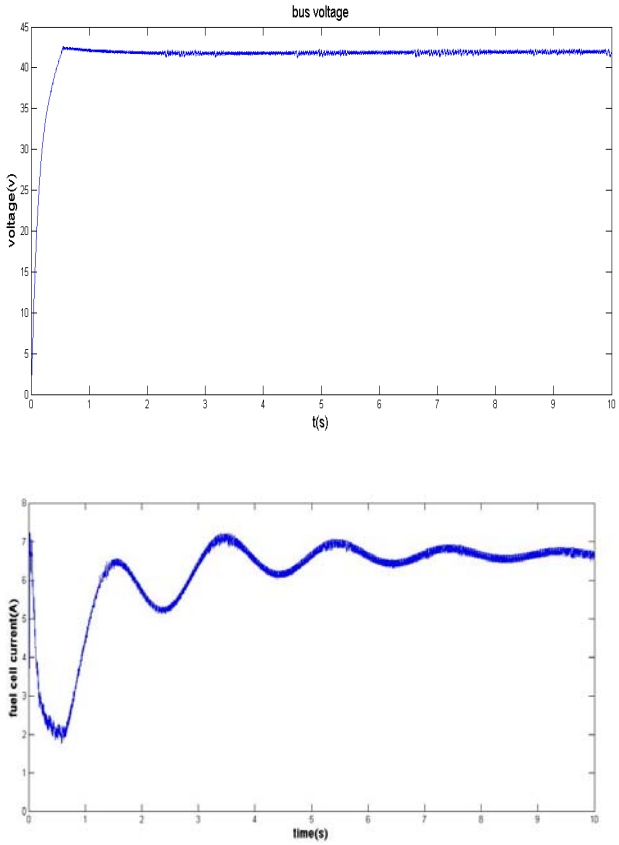

Fig.13 bus voltage and fuel cell current soft boost is used

REFERENCES

[1] Dr Peter Harrop,Military Electric Vehicles -Where, Why, What Next?, IDTechEx Ltd 2011

[2] 3757 w.touhy ave. ,Lincolnwood,il,6072,www.illcap.com.

[3] Zhenyuan Zhang, Wei-Jen Lee, *IEEE Fellow*, Meng Liu, PEM Fuel Cell and Battery Hybrid Power Supply System Design Based On Fuel Flow Rate Control, 978-1-4577-0365-2/11/$26.00 ©2011 IEEE

[4] JIANG Zhi-ling , CHEN Wei-rong , QU Zhi-jian , DAI Chao-hua, CHENG Zhan-li, Energy Management for a Fuel Cell Hybrid Vehicle, 978-1-4244-4813-5/10/$25.00 ©2010 IEEE.

[5] Seyoung Kim and Sheldon S. Williamson, *Member, IEEE*, Modeling, Design, and Control of a Fuel
Cell/Battery/Ultra-capacitor Electric Vehicle Energy Storage System.

[6] M.A. Hannan , F.A. Azidin , A. Mohamed, Multi-sources model and control algorithm of an energy management system for light electric vehicles, Energy Conversion and Management 62 (2012) 123–130.

[7] ned mohan,tore m.undeland,William p robbins,power electronics,converters,applications and design,john wiley& sons, inc,1989,ISBN 0-471-58408-8.

[8] Marselin Jamlaay,Dual Feedback Control DC-DC Boost ConverterBased on PI Controller, ISSN 2301-6132, IJEERI, VOL.2, NO. 1, MAR 2013

[9] Junhong Zhang, Bidirectional DC-DC Power Converter Design Optimization, Modeling and Control, Copyright 2008, Junhong Zhang

[10] Premananda Pany, R.K. Singh, R.K. Tripathi, Bidirectional DC-DC converter fed drive for electric vehicle system,international journal of engineeg,scince and technolog,vol.3,no.3,2011,pp.101.110

[11] lithiumion batteries data sheet(CGR18650 C)

[12] Andrew F. Burke Batteries and Ultracapacitorsfor Electric, Hybrid, andFuel Cell Vehicles, Vol. 95,No. 4, April 2007 IEEE

[13] Piyush Bubna, Suresh G. Advani, Ajay K. Prasad, Integration of batteries with ultracapacitors for a fuel cell hybrid transit bus,Journal of Power Sources 199 (2012) 360– 366

[14] JennHwa Wong , N.R.N.Idris , Makbul Anwari , Taufik Taufik, A Parallel Energy-Sharing Control for Fuel cellBattery-Ultracapacitor Hybrid Vehicle.

[15] Phatiphat Thounthong, Stephane Raël , Bernard Davat, Energy management of fuel cell/battery/super capacitor hybrid power source for vehicle applications, Journal of Power Sources 193 (2009) 376–385